The Effect of Molybdenum on V-Mg-O Catalysts in the Oxidative Dehydrogenation of Propane

A thesis submitted
in partial fulfillment of the requirements
for the degree of
Master of Technology

by
M. Mahesh

to
DEPARTMENT OF CHEMICAL ENGINEERING
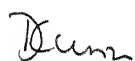**INDIAN INSTITUTE OF TECHNOLOGY KANPUR**
February, 2000

Certificate

This is to certify that the work contained in the thesis entitled *The Effect of Molybdenum on V-Mg-O Catalysts in the Oxidative Dehydrogenation of Propane*, by M. Mahesh, has been carried out under my supervision and that this work has not been submitted elsewhere for a degree.

Dr. D. Kunzru
Professor
Dept. Of Chemical Engg.
IIT, Kanpur.

28 February, 2000

ACKNOWLEDGEMENT

Mahesh

Contents

List of Figures

List of Tables

Abstract

A detailed study on the effect of molybdenum on V-Mg-O catalysts in the oxidative dehydrogenation (ODH) of propane has been performed. All the catalysts have been prepared using citrate method. It was found that the activity of the binary V-Mg-O ctalysts was higher for lower vanadium loading. So the active binary catalysts $V_1Mg_4O_x$ and $V_1Mg_9O_x$ have been selected for the doping with molybdenum and a detailed study has been carried out on $V_1Mg_9O_x$ catalyst. All the prepared catalysts have been characterized using X-Ray diffraction, surface area, Fourier transform infrared spectra and temperature programmed reduction. The reaction studies were carried out in a tubular quartz reactor at 773, 798 and 823 K under atmospheric pressure. It has been found that the incorporation of Mo modifies the number and reducibility of the active sites in V-Mg-O catalysts and thus the catalytic performance of the catalyst. The selectivities of the Mo-doped catalysts were found higher than that of the undoped catalysts, due to the decrease in the concentration of non-selective sites. However, the activity decreased with increasing molybdenum content. In this way, the best catalyst was obtained for a bulk Mo/V atomic ratio of 0.6. Finally, the effect of temperature was studied on $Mo_{0.6}V_1Mg_9O_x$ and $Mo_{0.3}V_1Mg_4O_x$ catalysts. It was also found that for a given conversion, higher temperatures give higher selectivity to propene.

Introduction

In petrochemical industry, light olefins like ethylene, propene and butylene are the major feedstock for a wide variety of chemicals such as acids, aldehydes and alcohols. The usual processes used for the manufacture of light alkenes are dehydrogenation of alkanes, steam cracking of naphtha and fluidized catalytic cracking of gas oil. Thermodynamically, the dehydrogenation process is favored at high temperature and low pressure. Catalytic dehydrogenation at such high temperatures results in undesirable side reactions such as cracking of the alkane into smaller molecule. One effect of this is rapid coking of the catalyst and it needs frequent regeneration. The steam cracking has also some disadvantages such as the high process temperature required, deposition of coke on the reactor walls and the higher energy requirement.

Oxidative dehydrogenation of alkane is one of the other alternatives to the above processes. The overall reaction of this process can be represented as

$$C_nH_{2n+2} + \frac{1}{2}O_2 \rightarrow C_nH_{2n} + H_2O$$
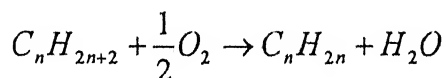
In this process, several parallel and consecutive reactions occur simultaneously, and in addition to the desired product (alkene), undesired products such as carbon oxides are also formed. The main advantage of this reaction is that the oxidation of the hydrogen evolved in the pure dehydrogenation to a very stable product,

water. In addition, the reaction is exothermic and is able to proceed at lower temperatures at which the formation of coke and cracking products are insignificant. One more advantage is that the conversion is no longer limited by thermodynamic factors and in practice complete conversion can be obtained even at low temperatures and high pressures.

In oxidative dehydrogenation, the key aspect is activating only the C-H bonds of the alkane molecule in the presence of oxygen. Activation of the weaker bonds in the presence of oxygen usually leads to the deep oxidation resulting in oxygenated products as well as carbon oxides. Therefore, the pathway of the reaction should be controlled to prevent deep oxidation or secondary reactions. The selective oxidation to alkenes is a major challenge as thermodynamically the formation of oxidation products such as carbon monoxide and carbon dioxide is favored. Hence the reaction should be controlled kinetically. Thus a catalyst is employed which will take care of the both the features and enhance the efficiency of the process. This process is essentially the catalytic oxidative dehydrogenation.

A lot of work has been in progress for the last decade to find out suitable catalysts for the oxidative dehydrogenation of light alkanes. A wide variety of catalytic systems have been studied. Of all these, vanadium based oxides have been found to be the most effective catalysts. Vanadium-magnesium mixed oxide (V-Mg-O) catalytic system is reported to be active and selective for oxidation of C_2-C_4 alkanes [1-6]. Till now, very little work has been reported on multicomponent catalysts.

1.1. Objectives

The main objective of the present study was to investigate the activity and selectivity of the V-Mg-O and V-Mo-Mg-O catalysts and to compare the performance of these catalysts. Another objective was the characterization of these catalysts using various techniques such as X-Ray diffraction (XRD), Fourier transform infrared spectra (FTIR), temperature programmed reduction (TPR) and surface area.

Literature Review

Oxidative dehydrogenation is a potentially attractive method for converting light alkanes to the corresponding alkenes. During the last decade, research has been intensified in this direction. A wide variety of catalysts have been reported in the literature for the ODH of ethane, propane and butane. The majority of the work has involved catalysts in which vanadium is one of the components. However, most of the work has been limited to either single metal oxides or binary catalysts consisting of mixed metal oxides.

2.1. Binary catalysts

Many of the studies on the ODH of propane have been reported on binary catalysts of various combinations. Corma et al. [1] studied the ODH of propane over vanadium supported on various metal oxides like SiO_2, Al_2O_3, TiO_2, MgO, La_2O_3, Sm_2O_3 and Bi_2O_3 as well as on La, Sm and Bi orthovanadates. Their results showed that stronger the basicity of the support, higher was the selectivity to propene. They postulated that the use of basic metal oxide induced the formation of tetrahedral V^{5+} species selective to ODH and the number of VO^{2+} species, which strongly hold propene leading to deep oxidation, are lower. In another study, Barbara [2] has shown that the structure and properties of dispersed species were influenced by the type of support : the basic and amphoteric oxides favor the bidimensional dispersion, whereas the acidic ones, the formation of tridimensional microunits of V_2O_5. Albonetti et al. [3] concluded that the acidity as well as basicity of the catalysts favored desorption of the products - basicity in case of olefins and acidity in case of acids and anhydrides. To minimize the side

reactions, they suggested the use of basic or neutral catalysts so that the desorption of olefins was faster, thus minimizing the side reactions.

Magnesium oxide was the obvious choice as support for most of the workers. Interestingly it was shown that the Mg orthovanadate was the only alkali or alkaline earth orthovanadate selective to propene. Ca, Sr, Ba, Li and Cs orthovanadates were nonselective. It was explained that except for $MgCO_3$, which decomposes at about 400 ^0C, the high thermal stability of other carbonates results in disintegration of their orthovanadates into carbonates and vanadium oxide under reaction conditions to become nonselective catalysts [4].

The effect of vanadium loading on the catalytic performance has been studied over a wide range of vanadium content. In a review paper [5], Mamedov et al. summarized the data published till 1994 on the vanadium-based catalysts in the ODH of C_2-C_5 alkanes. The discussed data showed that dehydrogenation selectivity was improved for low vanadium loading, because of presence of isolated tetrahedral species (VO_4 groups). These VO_4 groups in orthovanadate are expected to be reduced to a smaller extent as their oxygen ions are more difficult to remove than those in V_2O_7 units in pyrovanadates. An optimum extent of reduction and hence a good selectivity can be achieved either by carrying out the reaction under more severe conditions i.e. at higher temperatures and/or at larger alkane to oxygen ratio or by using more reactive alkane. The specific activity increased with vanadium loading within the monolayer coverage. At higher loading vanadium atoms are inserted in a V_2O_5 lattice, which is not accessible for reaction. Most of the workers reported that lower vanadium oxide loading of 15-40wt% resulted in active catalysts with magnesium orthovanadate ($Mg_3V_2O_8$) as the active phase. In contrast, Sam et al. [6] claimed that intermediate vanadium content of 40-70 wt% provided the most selective catalysts with magnesium pyrovanadate ($Mg_2V_2O_7$) as the active phase. Chaar et al. [7] found that $Mg_3V_2O_8$ phase was most active and selective for the ODH of propane. On the other hand, some studies suggest that $Mg_2V_2O_7$ was responsible for high selectivity and $Mg_3V_2O_8$ was responsible for total oxidation [6, 8].

The influence of precursors of V-Mg-O catalysts on their properties by using different MgO precursors was studied by Corma et al. [9]. They found that the phase formation was controlled by the preparation procedure. The influence of the preparation method (impregnation, aqueous/non-aqueous, citrate method, vapor phase grafting) on the properties of catalysts has been studied on different catalysts. Calcination temperature also plays a vital role on the properties of the catalysts. Increase in calcination temperature of some catalysts (60 VMgO, having 60wt% V_2O_5) resulted in narrow peaks of the orthovanadates [6], whereas at lower temperatures broad peaks were observed with possible distorted structure of the orthovanadate. In some cases, it was reported that pure phases could be obtained by the use of high temperatures while lower temperatures resulted in incomplete transformation and presence of mixed phases.

In an interesting study, Gao et al. [10] found that the citrate method could be used to prepare all the three pure Mg vanadates. Among all the three phases, $Mg_2V_2O_7$ was found to be most selective and MgV_2O_6 the least. They also found that the selectivity of the $Mg_3V_2O_8$ could be increased by coexisting pyrovanadate phase or magnesium oxide. Carrazan et al. [11] studied the synergetic effects of the mechanical mixtures of all the three Mg vanadate phases. All the pure Mg vanadate phases were prepared using citrate method. They found that $Mg_3V_2O_8$ was the most active phase while $Mg_2V_2O_7$ was the most selective phase. The selectivity of $Mg_3V_2O_8$ was improved when it was mechanically mixed with the selective phase, $Mg_2V_2O_7$. This was attributed to the synergetic effect between the phases.

The effect of homogeneous reaction during the catalytic ODH of alkanes can be significant at high temperatures (>873 K). Burch and Crabb [12] studied in detail the role of homogeneous and heterogeneous reactions in ODH of propane. The conversion vs. selectivity relationships for both the homogeneous and most of the heterogeneous reactions were found to be similar though the homogeneous reactions required a higher temperature. They suggested that a combination of homogeneous and heterogeneous contribution to the reaction may provide a means of obtaining higher yields of propane. Kung and Nguyen [13] have also shown the importance of

homogeneous reactions in the pre and post catalytic volume of the reactor. Delmon et al. [14] have studied the beneficial effect of water in homogeneous reaction of propane ODH.

Walting et al. [15] studied the ODH of propane over niobia supported vanadium oxide catalysts. They reported that the selectivity to propylene strongly depends on the nature of the catalyst as readsorption and interaction of propene with the acid sites leads to total oxidation. They concluded that the optimization of weak sorption of propene is the key factor for the design of the selective oxidative dehydrogenation catalysts. Young et al. [16] studied ODH of propane over magnesium molybdate catalysts and reported that $Mg_{0.95}MoO_x$ showed the highest activity. They also concluded that lattice oxide ions of the catalyst surface act as active oxygen species for the ODH of propane.

2.2. Multicomponent catalysts

The addition of a suitable third metal oxide to the binary catalysts can improve the existing interaction between the metal oxides and can promote the migration of the lattice oxygen. Therefore, the preparation of optimal catalysts should include the presence of metallic elements, which will be able to change the valence states in the redox reactions. In this way, different transition metal compounds have been studied to modify the performance of binary catalysts. However, the information available on multicomponent catalysts is rather scanty as compared to the binary catalysts.

Valenzuela et al. [17] studied the effect of the addition of K_2O, Cr_2O_3, Sm_2O_3 and Nb_2O_5 to the V-Mg-O catalyst on the ODH of propane. They reported a decrease in both the activity and selectivity due to the doping of these metal oxides. They found that the most easily reduced catalyst was the most selective. Carrazan et al. [11] studied the ODH of propane on V-Sb-Mg-O impregnated catalysts and on mechanical mixtures of Mg-vanadates with Sb-oxide. Synergetic effects were observed in

$Mg_3V_2O_8$ and $Mg_2V_2O_7$ when these were mixed with α-Sb_2O_4. In the case of $Mg_3V_2O_8$, propane conversion decreased with increasing Sb loading while the selectivity increased. On the other hand, conversion and yield increased with increasing Sb loading for $Mg_3V_2O_8$ while the selectivity decreased. Cadus et al. [36] studied the ODH of propane over $MgMoO_4$-MoO_3 catalysts. They reported a significant synergetic effect between the phases with a propene selectivity of 91% at 10% propane conversion.

Lopez et al. [18] studied the ODH of ethane on vanadium containing binary and ternary oxides supported on alumina. The activity and selectivity for the oxides such as NiV, CoV, SnV and SbV supported on alumina was nearly same, whereas ternary systems such as NiVSb, CoVSb, SnVSb and BiVSb supported on alumina showed notably different catalytic behaviours. They reported that SnVSb was the most active while NiVSb was the most selective. The highest selectivity to ethylene of up to 80% was characteristic of the NiVSb system. Valenzuela et al. [19] have also studied the alumina supported NiV, SbV and NiVSb oxides for the ODH of ethane. They found that the most easily reduced NiVSb system was the most selective and proposed that the reaction occurred through a redox mechanism. The selectivity to ethylene followed the order similar to that for surface reducibility, i.e. NiVSb > SbV >NiV. The absence of free NiO and V_2O_5 in the ternary system was explained for its better selectivity. Thorsteinson et al. [20] investigated mixed oxide catalysts containing Mo and V (MoV) together with another transition metal oxide (Ti, Cr, Mn, Fe, Co, Ni, Nb, Ta or Ce) in the ODH of ethane. Burch et al. [21] studied the ODH of ethane on Mo/V/Nb oxide catalysts. They reported that addition of niobium had a dual role. One, it combined with free MoO_3 or V_2O_5 and thus eliminated the total oxidation sites. Secondly it formed a new mixed oxide phase, which contained active and selective sites for the ODH of ethane.

Stern et al. [22] studied the effect of addition of different promoters like Mo, W, B, Al, Ga, Sb and SbP on Mg-V-oxide based catalysts in the ODH of n-butane. They reported that Sb, SbP and B promoted systems were twice as selective as the V-Mg-O catalysts at comparable conversions. The improved selectivity was attributed to the formation of ternary phases. Ga and Al containing V-Mg-O catalysts were the most

active while the W containing system was the only one yielding detectable amounts of furan. Bhattacharyya et al. [23] studied the effect of different promoters viz. Cr_2O_3, MoO_3 and TiO_2 on the performance of V-Mg-O catalysts. They found that Cr_2O_3 and MoO_3 enhanced the activity of the V-Mg-O system, while TiO_2 enhanced the selectivity. A better yield of butadiene on promoted V-Mg-O system was obtained in comparison to the unpromoted V-Mg-O system.

Dejoz et al. [24] studied the role of molybdenum in Mo-doped V-Mg-O catalysts during the ODH of butane. The selectivity to ODH products increased with increasing molybdenum content up to Mo/V atomic ratio of 0.6 and then decreased for higher Mo-content. The incorporation of molybdenum improved the selectivity of the ODH products by decreasing the non-selective sites related to vanadium-free magnesia on the surface. At constant conversion, higher selectivities were obtained at higher reaction temperature. They attributed this to the higher activation energy for the ODH reactions compared to the activation energies for the formation of carbon oxides.

Oganowski et al. [25] studied the effect of Mo, Cr and Co on V-Mg-O catalyst system in the ODH of ethylbenzene to styrene. They showed that molybdenum doping improved the selectivity whereas chromium and cobalt improved the activity of the V-Mg-O system. The quaternary oxide system V-Cr-Co-Mg-O was found to give the best performance.

Smits [26] investigated the ODH of propane on niobia by doping it with various transition metals. The addition of Pb or Sb caused a decrease in the niobia activity while the addition of other metals viz. Mo, Cu, Fe, Co, Ni, Mn, Cr and V increased the activity of niobia. Of all, V-Cr-Nb-O system was reported to be especially suitable as the selectivity to propylene remained high with increase in the activity of niobia. Viparelli et al. [27] studied the ODH of propane over vanadium and niobium supported catalysts. They reported an increase in the selectivity of the catalyst with increasing niobium content.

The available literature clearly shows that the V-Mg-O system is the most effective catalyst for the ODH of propane and doping can significantly alter the properties of the V-Mg-O catalyst. In the present study the effect of molybdenum on V-Mg-O catalytic system has been studied in detail.

Experimental Details

3.1. Catalyst Preparation

3.1.1. Preparation of binary catalysts

Magnesia supported vanadium oxide catalysts were prepared using citrate method. This method was used by Gao et al. [10] to prepare pure phases of Mg vanadates. The advantages of this method are : (a) the expected oxide compounds can be obtained from very homogeneous citrate precursors, and (b) lower calcination temperatures can be used. In this method first a transparent solution of magnesium nitrate (99% purity, E. Merck (India) Limited, Mumbai) was prepared in demineralised water. Ammonium metavanadate (Reanal, Budapest) was added to the solution in the desired Mg/V atomic ratio. Then citric acid (99.5% purity, E. Merck (India) Limited, Mumbai) was added in such a proportion that 1.1 equivalent-gram of acid function per valence-gram of metal was present in the solution. The clear solution was evaporated in rotavaporator at 50 ^{0}C to obtain a viscous solution. The viscous solution was then dried in an oven at 120 ^{0}C for 15 hours. The amorphous organic compound obtained was powdered and finally calcined at 550 ^{0}C for 6 hours. The final catalyst powder obtained was light yellow in color. An increase in the intensity of the yellow color was observed with increasing Mg/V ratio.

In most of the published studies it has been reported that among the three pure phases of V-Mg-O catalysts, $Mg_3V_2O_8$ (Mg/V atomic ratio of 3/2 or V_2O_5wt% of

60) is most active and $Mg_2V_2O_7$ (Mg/V atomic ratio of 2/2 or V_2O_5wt% of 70) is most selective. In some papers it has been reported that V-Mg-O catalyst containing 19wt% V_2O_5 (rest MgO, Mg/V atomic ratio 9.67) is the most effective for the ODH of propane. Murty [28] and Malge [29] also confirmed this. Therefore to study the V-Mg-O catalysts 5 different catalysts with V_2O_5 content ranging from 20 to 70wt% were prepared. The catalysts have been denoted as $V_xMg_yO_z$. The Mg/V atomic ratios and the V_2O_5 wt% of the binary catalysts prepared are given in Table 3.1.

3.1.2. Preparation of Mo-V-Mg-O catalysts

Molybdenum doped ternary catalysts were also prepared using the citrate method. For the preparation of these ternary catalysts, ammonium heptamolybdate (99.0% purity, E. Merck (India) Limited, Mumbai) was used as the precursor for the molybdenum. Ammonium heptamolybdate in the desired Mo/V atomic ratio was added to the solution of magnesium nitrate and ammonium metavanadate. The solution was evaporated in rotavaporator at 50 ^{0}C and the paste was dried and calcined under similar conditions as used for the binary catalysts. Catalyst samples with Mo/V atomic ratio varying from 0.1 to 1.0 were prepared. The catalysts have been denoted as $Mo_aV_bMg_cO_d$.

3.2. Experimental Apparatus

The experimental set up basically consists of mass flow controllers, a mixing chamber, reactor and chromatographs equipped with data station. The schematic diagram of the apparatus is shown in Figure 3.1. The standard feed composition was 4 mol% propane, 8 mol% oxygen and 88 mol% nitrogen. Nitrogen was first passed through pyragallol solution to remove any traces of oxygen present in the gas, and then through a silica gel column to remove the moisture. The flow rates of nitrogen, oxygen and propane were controlled by using three mass flow controllers (Model 8270, Matheson, USA for nitrogen; Model ISO 9001, Bronkhorst, Netherlands for oxygen and propane). All the

three gases were combined and passed through a mixer for effective mixing and then sent to the reactor.

The quartz reactor was 350 mm in length with an internal diameter of 10 mm. Another quartz tube of 300 mm in length with an internal diameter of 3.0 mm was attached at the bottom of the reactor to facilitate fast removal of the products. The reactor was mounted vertically in the middle of a tubular furnace of 500 mm in length. Quartz wool inserted at the constriction served as the catalyst support. The top of the rector was connected to the gas line using 1/8" Swagelock fittings and specially machined unions made of aluminum. Power to the furnace was supplied through a 15A variac and the temperature of the furnace was controlled using a proportional temperature controller (Model IT 401-D2, Indotherm, Mumbai). The axial temperature profile in the reactor was measured using a chromel-alumel thermocouple inserted in a stainless steel thermowell (O.D. 3.0 mm).

The effluent gas stream from the reactor was bifurcated and the two streams were passed through the sampling valves of two online chromatographs connected to a data station. A computer was connected to the data station to store the chromatograms and their peak areas.

3.3 Experimental Procedure

The catalyst powder obtained after the calcination was pelletized, crushed and sieved to obtain a fraction of size 250-500 μm. The mass of the catalyst used in the reactor was varied depending on the performance of the catalyst. Initially for all the catalysts, 200 mg of the sample was used. To reduce the thermal effects during the reaction, the catalyst was diluted with 500 μm quartz particles. The mass fraction of the active catalyst was usually 20% (rest quartz). For all the runs, the total bed volume was kept the same ($\sim$1.2 cm^3) so that when the mass of the catalyst was changed then the mass of the quartz particles was also changed to maintain a fixed bed height. The thoroughly

mixed mass of catalyst and quartz particles was placed in the reactor on a quartz wool support. A layer of quartz wool was again placed on the top of the catalyst bed to prevent disturbances to the bed while handling. The remaining volume of the reactor was filled with quartz chips. The themowell was then placed co-axially in the center such that its tip touched the quartz wool supporting the catalyst bed. The loaded reactor was then placed in the furnace and the gas line was connected using Swagelock fittings.

Before the reactor heating was started, the feed gas sample was analyzed. For this all the three gases were fed at the desired flow rates through the cold reactor. After stabilization of the flow, the sample was analyzed by injecting into the two chromatographs using sampling valves. Then the furnace was heated up to the desired temperature and system was left for stabilization for 90 min before the samples were injected into the chromatographs for the analysis of the products. At each temperature the samples were taken at an interval of 90 min. Atleast two samples were taken for the analysis at a particular temperature. The total run time at each temperature was usually 4 h including the 1 hr for stabilization after changing the temperature. The runs were taken either by changing the temperature at a particular flow rate or by changing the flow rate at a constant temperature.

3.4. Product Analysis

The product gases were analyzed by gas chromatography using two columns namely Carbosphere and Molecular Sieve 5A in two separate chromatographs. A Carbosphere column (length 1.83 m, I.D. 2.0 mm) connected with a methanizer was used to separate carbon monoxide, methane, carbon dioxide, propylene and propane using flame ionization detector (FID) in one chromatograph (Model 5700, Nucon). Nitrogen at 30 ml/min was used as the carrier gas. The injector, methanizer and detector were maintained at 373, 583 and 423 K respectively. The oven temperature was programmed such that carbon monoxide, methane and carbon dioxide were detected at an isothermal temperature of 45 ^{0}C and propylene and propane were detected at a

temperature of 200 ^{0}C. In the programmed mode the oven was kept initially at 45 ^{0}C for about 20 min and then heated up to 200 ^{0}C at a rate of 20 ^{0}C/min. It was kept at 200 ^{0}C for about 20 min and then brought back to initial temperature for analyzing the next sample. A Molecular Sieve 5A column (length 2 m, I.D. 2.0 mm) was used to separate oxygen and nitrogen using thermal conductivity detector (TCD) in another chromatograph (Model 5765, Nucon). Helium at 30 ml/min was used as the carrier gas. The filament current was 150 mA. All the chromatograms were stored in a computer using a data station (Aimil Chromatography) connected between the chromatographs and the computer. The areas obtained were converted into the mole ratios using the corresponding calibration factors of the product compounds (Appendix 1). The calibration factors were obtained using a standard gas mixture (MultiTech, New Delhi).

Table 3.1. Atomic ratios of Mg/V and V_2O_5wt% of the binary catalysts.

Catalyst	Mg/V atomic ratio	V_2O_5 wt%
$V_2Mg_2O_x$ ($Mg_2V_2O_7$)	2/2	69.47
$V_4Mg_5O_x$	5/4	64.54
$V_2Mg_3O_x$ ($Mg_3V_2O_8$)	3/2	60.28
$V_1Mg_4O_x$	4/1	36.23
$V_1Mg_9O_x$	9/1	20.05

1. Nitrogen cylinder
2. Oxygen cylinder
3. Propane cylinder
4. Nitogen flow controller
5. Oxygen flow controller
6. Propane flow controller
7. Pyragallol solution
8. Silica gel trap
9. Mixer
10. Manometer
11. Bypass line
12. Quartz reactor
13. Furnace
14. Thermowell
15. Thermocouple
16. Collector
17. Sampling valve

To FID   To TCD

Exit
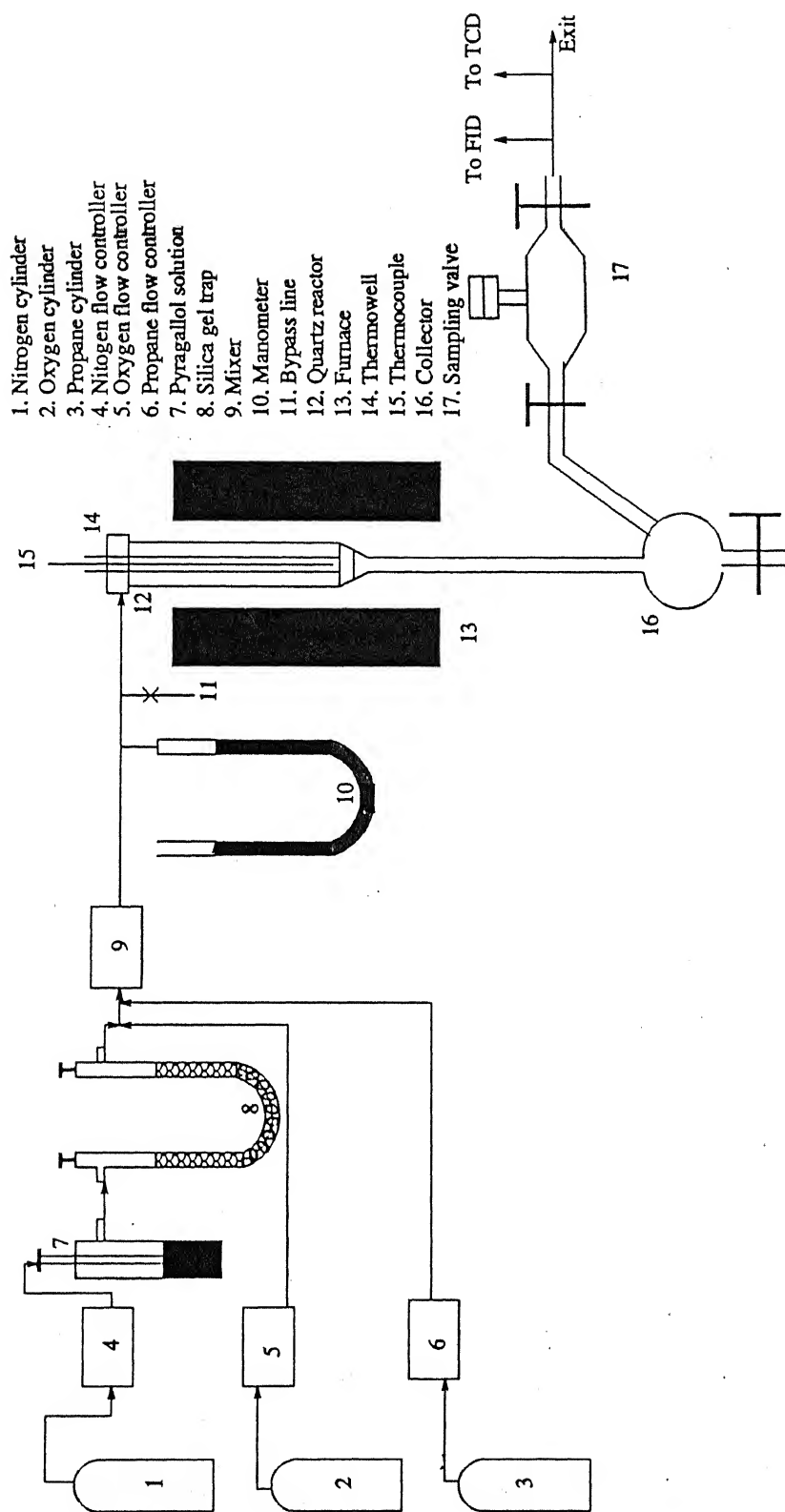
Figure 3.1 Schematic diagram of experimental setup

<div align="right">

4

Characterization

of Catalysts

</div>

The primary purpose of characterization is to provide a basis for understanding the interrelationship between activity and selectivity of a catalyst and its physical and chemical properties. The catalysts were characterized using X-Ray diffraction (XRD), surface area, Fourier Transform Infrared (FT-IR) spectroscopy and temperature programmed reduction (TPR).

4.1. Phase Composition of Catalysts

X-Ray diffraction was used to identify the crystalline phases in a catalyst. The atoms and ions, which are the chemical building blocks of the substance, are arranged in a three dimensional structure. X-Rays, incident on a crystalline solid, are diffracted due to elastic scattering of the ray quanta on the electrons of these chemical building blocks. The lattice structure, therefore, can be related to the resulting diffraction pattern. The spectra of the samples were obtained on a Reich Seifert (Germany) Iso Debye Flex 2002 X-Ray diffractometer using Cu Kα radiation of wavelength 1.5406 ^{0}A. The resulting diffraction peaks were recorded on a Servogor 300 chart recorder. For the analysis, the powdered samples were placed in the sample plate of the diffractometer. The $'d'$ values for the catalyst samples were calculated using Bragg's law

$$n\lambda = 2d \sin \theta \qquad [1]$$

where θ is the angle of the incidence with respect to a set of lattice planes (h, k, l); λ is the wavelength of incident radiation and n is the order of diffraction. The value of n was

taken as one in the calculation of $'d'$ values. Qualitative analysis of the resulting spectra were done by comparing the calculated values of $'d'$ with the standard values from the powder diffraction files [31].

The results of XRD studies of the catalysts are tabulated in Tables 4.1-4.13. For the binary catalysts having higher vanadia content, prominent peaks corresponding to the pure phases of $V_2Mg_2O_7$ and $V_2Mg_3O_8$ were observed. Table 4.1 shows the $'d'$ vs. intensity values obtained from the XRD spectra of $V_2Mg_2O_x$ catalyst. These values are in good agreement with the standard values for $Mg_2V_2O_7$ phase. Similarly the $'d'$ values obtained from the XRD spectra of $V_2Mg_3O_x$ (Table 4.2) were in good agreement with the standard values for $Mg_3V_2O_8$ phase. In case of $V_4Mg_5O_x$ system (Table 4.3), both the phases $Mg_3V_2O_8$ and $Mg_2V_2O_7$ were observed. Besides these two phases, minor amounts of V_3O_5 and MgO phases were also present. The XRD spectra of the above mentioned three catalysts were in good agreement with those reported by Gao et al. [10].

For the catalysts $V_1Mg_4O_x$ and $V_1Mg_9O_x$ strong reflection lines corresponding to the MgO phase were observed. In addition, some broad peaks due to Mg orthovanadate were also detected with low intensities. This is in good agreement with the results reported by Sam et al. [6] and Valenzuela et al. [17]. In their study, the XRD patterns for the catalysts having higher Mg content showed only the presence of MgO and no other peaks of possible compounds of V-Mg-O were detected due to their low concentration in the solid. For all the catalysts, the $'d'$ values of the phases were in good agreement with standard values. However, the measured intensity ratios were very low compared to the standard values, which indicates that the sample has a lower crystallinity. In some cases (refer Table 4.3, 4.8, 4.13), intensity ratios were higher than the standard values, which could be because of the differences in measuring intensity of peaks and/or due to interference from another crystalline phase. This problem was further aggravated by peak broadening. For V-Mg-O catalysts, the poor resolution and the broadening of the peaks has been attributed to high dispersion and a possible distorted structure of orthovanadate phase [30].

Most of the ternary catalysts showed magnesium oxide as the major phase (refer Table 4.6-4.13). For ternary catalysts, the intensity of the MgO peaks reduced due to the formation of additional phases with Mg. Some catalysts showed the broad peaks of $Mg_3V_2O_8$ phase in addition to the magnesium oxide. The intensity of the MgO peaks was reduced with increasing Mo/V atomic ratio. The ternary catalysts $Mo_{1.0}V_1Mg_4O_x$ and $Mo_{1.0}V_1Mg_9O_x$, with a Mo/V atomic ratio of 1.0 showed the presence of α-$MgMoO_4$. No other peak of appreciable intensity was present in any of the ternary catalysts. This is in good agreement with the phases recognized by Dejoz et al. [24] in Mo doped V-Mg-O catalysts prepared by impregnation method.

Most of the catalysts in the present study were X-ray amorphous. Though it can be expected that some of the phases like magnesium orthovanadate and magnesium molybdate could exist in all the ternary catalysts prepared, they could not be detected by XRD possibly due to lower crystallinity or lower concentration of these phases. Another reason for the line broadening could be that the size of the crystalline particle might be in the range of 3-50 nm [32].

Table 4.1 Phase composition of $V_2Mg_2O_x$ ($Mg_2V_2O_7$)

Calculated value		Standard values		Phase present
$d, {}^0A$	I	$d, {}^0A$	I	
4.766	25.74	4.714	16	$Mg_2V_2O_7$
4.168	18.69	4.124	20	$Mg_2V_2O_7$
3.705	34.78	3.703	30	$Mg_2V_2O_7$
3.229	63.75	3.199	100	$Mg_2V_2O_7$
3.108	90.00	3.184	75	$Mg_2V_2O_7$
3.016	100	3.166	35	$Mg_2V_2O_7$
1.496	57.5	1.490	39	MgO
2.102	27.5	2.106	100	MgO
2.681	42.5	2.638	100	V_3O_5
2.896	100	2.870	70	V_3O_5

Table 4.2 Phase composition of $V_2Mg_3O_x$ ($Mg_3V_2O_8$)

Calculated values		Standard values		Phase present
$d, {}^0A$	I	$d, {}^0A$	I	
3.267	64.89	3.284	70	$Mg_3V_2O_8$
3.003	72.34	3.009	50	$Mg_3V_2O_8$
2.896	100	2.862	57.45	$Mg_3V_2O_8$
2.543	100	2.549	100	$Mg_3V_2O_8$
2.495	95.75	2.493	50	$Mg_3V_2O_8$
2.069	51.06	2.079	35	$Mg_3V_2O_8$

Table 4.3 Phase composition of $V_4Mg_5O_x$

Calculated values		Standard values		Phase
$d, {}^0A$	I	$d, {}^0A$	I	present
3.215	90.67	3.199	100	$Mg_2V_2O_7$
3.187	90.67	3.184	75	$Mg_2V_2O_7$
3.028	94.67	3.166	35	$Mg_2V_2O_7$
2.862	56	2.870	70	V_3O_5
2.675	37.33	2.638	100	V_3O_5
2.549	100	2.543	100	$Mg_3V_2O_8$
2.495	85.33	2.493	50	$Mg_3V_2O_8$
2.081	54.67	2.079	35	$Mg_3V_2O_8$
1.797	28	1.795	15	$Mg_3V_2O_8$

Table 4.4 Phase composition of $V_1Mg_4O_x$

Calculated values		Standard values		Phase
$d, {}^0A$	I	$d, {}^0A$	I	present
2.103	100	2.106	100	MgO
1.486	71.96	1.489	39	MgO
2.712	98.94	2.638	100	V_3O_5

Table 4.5 Phase composition of $V_1Mg_9O_x$

Calculated values		Standard values		Phase
$d, {}^0A$	I	$d, {}^0A$	I	present
2.548	44.74	2.549	100	$Mg_3V_2O_8$
2.494	42.11	2.493	50	$Mg_3V_2O_8$
2.102	100	2.106	100	MgO
1.489	61.84	1.489	39	MgO
1.221	25	1.216	10	MgO

Table 4.6 Phase composition of $Mo_{0.1}V_1Mg_4O_x$

Calculated values		Standard values		Phase present
$d, {}^0A$	I	$d, {}^0A$	I	
2.555	58	2.549	100	$Mg_3V_2O_8$
2.107	100	2.106	100	MgO
1.479	39	1.489	39	MgO

Table 4.7 Phase composition of $Mo_{0.3}V_1Mg_4O_x$

Calculated values		Standard values		Phase present
$d, {}^0A$	I	$d, {}^0A$	I	
2.527	64.10	2.549	100	$Mg_3V_2O_8$
2.112	100	2.106	100	MgO
1.478	94.87	1.489	39	MgO

Table 4.8 Phase composition of $Mo_{0.6}V_1Mg_4O_x$

Calculated values		Standard values		Phase
$d, {}^0A$	I	$d, {}^0A$	I	present
3.299	100	3.284	70	$Mg_3V_2O_8$
2.527	62.86	2.549	100	$Mg_3V_2O_8$
2.083	82.86	2.106	100	MgO
1.485	88.57	1.489	39	MgO

Table 4.9 Phase composition of $Mo_1V_1Mg_4O_x$

Calculated values		Standard values		Phase
$d, {}^0A$	I	$d, {}^0A$	I	present
3.299	100	3.330	100	α-$MgMoO_4$
2.527	35.62	2.549	100	$Mg_3V_2O_8$
2.083	39.04	2.106	100	MgO
1.485	37.61	1.489	39	MgO

Table 4.10 Phase composition of $Mo_{0.1}V_1Mg_9O_x$

Calculated values		Standard values		Phase present
$d, {}^0A$	I	$d, {}^0A$	I	
2.548	39.76	2.549	100	$Mg_3V_2O_8$
2.494	40.96	2.493	50	$Mg_3V_2O_8$
2.102	100	2.106	100	MgO
1.489	60.24	1.489	39	MgO
1.218	25.30	1.216	10	MgO

Table 4.11 Phase composition of $Mo_{0.3}V_1Mg_9O_x$

Calculated values		Standard values		Phase present
$d, {}^0A$	I	$d, {}^0A$	I	
2.102	100	2.106	100	MgO
1.489	62.32	1.489	39	MgO
1.217	26.09	1.216	10	MgO

Table 4.12 Phase composition of $Mo_{0.6}V_1Mg_9O_x$

Calculated values		Standard values		Phase present
$d, {}^0A$	I	$d, {}^0A$	I	
2.093	100	2.106	100	MgO
1.483	73.68	1.489	39	MgO
1.217	29.03	1.216	10	MgO

Table 4.13 Phase composition of $Mo_1V_1Mg_9O_x$

Calculated values		Standard values		Phase present
$d, {}^0A$	I	$d, {}^0A$	I	
3.897	43.03	3.860	100	α-$MgMoO_4$
3.119	54.72	3.140	60	α-$MgMoO_4$
2.102	100	2.106	100	MgO
1.483	75.47	1.489	39	MgO
1.218	30.03	1.216	10	MgO

4.2. Measurement of Specific Surface Area

The surface areas of all the catalyst samples were measured using single point BET method by the physisorption of nitrogen at liquid nitrogen temperature (77 K). The studies were carried out on a Micrometrics Pulse Chemisorb 2700 unit based on dynamic adsorption technique. The samples were first prepared by heating up to 623 K in an inert atmosphere to remove any adsorbed species from the surface of the catalyst. Helium was used as the inert gas. Then test gas consisting of 30mole% nitrogen in N_2-He mixture was passed through the sample. After the stabilization of flow the sample was covered by a bath of liquid nitrogen to condense the nitrogen in the test gas into the pores of the catalyst. The condensed nitrogen gas was then desorbed by immersing the sample in a water bath.

The specific surface areas of all the catalyst samples are tabulated in Table 4.14. As can be observed from this table, the surface areas of the VMgO catalysts decreased with decreasing magnesium content. The surface area of the binary catalytic system gradually decreased from 150.8 to 8.4 m^2/g as the Mg/V atomic ratio of the catalyst decreased from 9/1 to 1/1. This decreasing trend is in good agreement with the literature results [10]. The surface areas of the binary catalysts of the present study were higher than those prepared using the impregnation method.

In the case of ternary catalysts, the surface areas of the molybdenum doped catalysts were found to be less than that of the undoped catalysts. Moreover, the surface areas of the catalysts decreased gradually with increasing molybdenum content. For the catalytic system $Mo_yV_1Mg_9O_x$, the surface area decreased from 150.8 to 64.2 m^2/g as the Mo/V atomic ratio increased from 0 to1.0. A similar effect of Mo-doping on surface area of VMgO catalyst has been reported earlier [24].

A possible explanation for the decrease in the surface areas of the doped samples could be the blocking of the pores by the added species. The high surface areas for all the catalysts of the present study could be due to the small average crystallite size of the samples, which is supported by the relatively blunt and distorted XRD patterns.

Table 4.14 Surface Areas of Catalysts

Catalyst	Surface area, m^2/g
$V_2Mg_2O_x (Mg_2V_2O_7)$	8.4
$V_4Mg_5O_x$	24.1
$V_2Mg_3O_x (Mg_3V_2O_8)$	29.7
$V_1Mg_4O_x$	79.8
$V_1Mg_9O_x$	150.8
$Mo_{0.1}V_1Mg_4O_x$	67.4
$Mo_{0.3}V_1Mg_4O_x$	42.7
$Mo_{0.6}V_1Mg_4O_x$	37.5
$Mo_{1.0}V_1Mg_4O_x$	31.0
$Mo_{0.1}V_1Mg_9O_x$	130.3
$Mo_{0.3}V_1Mg_9O_x$	94.6
$Mo_{0.6}V_1Mg_9O_x$	71.1
$Mo_{1.0}V_1Mg_9O_x$	64.2

4.3. Fourier Transform Infrared (FT-IR) Analysis

Infrared spectra of the catalysts were obtained at room temperature on a Brucker Vector 22 spectrometer equipped with data station. 100 mg of the sample was thoroughly ground and mixed with dry KBr and pressed into a disk. The disk was then exposed to the infrared rays and the spectra consisting of peaks of the absorbance vs. wave number was obtained.

The FT-IR spectra of the binary catalysts showed the presence of $Mg_2V_2O_7$ and $Mg_3V_2O_8$ phases. For the catalyst $V_2Mg_2O_x$ intense bands were observed at 976, 920, 854, 828 and 440 cm^{-1}, which indicate the presence of Mg pyrovanadate phase [10]. For the catalyst $V_2Mg_3O_8$ peaks observed at 849 and 690 cm^{-1} [24] could be assigned to the presence of $Mg_3V_2O_8$. In $V_4Mg_5O_x$ catalyst both the phases $Mg_2V_2O_7$ and $Mg_3V_2O_8$ were observed. For the catalysts $V_1Mg_4O_x$ and $V_1Mg_9O_x$ having lower vanadia content, peaks observed at 856 and 671 cm^{-1} could be assigned to the $Mg_3V_2O_8$ phase. The bands observed at 435 and 422 might be due to MgO as both these catalysts have high Mg content. The FT-IR spectra obtained for $V_2Mg_2O_x$, $V_2Mg_3O_x$ and $V_4Mg_5O_x$ are in very good agreement with the results reported by Gao et al. [10]. The spectra of these samples are given in Figure 4.1, 4.2 and 4.3, respectively.

The FT-IR results of the ternary catalysts $Mo_{1.0}V_1Mg_4O_x$ and $Mo_{1.0}V_1Mg_9O_x$ are shown in Figures 4.4 and 4.5 respectively. When compared to the undoped catalysts, additional band was observed at 826 cm^{-1}, which indicates the presence of magnesium molybdate [24] in the ternary catalysts having higher molybdenum content. However, this phase was not found in the other ternary catalysts of lower Mo/V ratio. This was in confirmation with the XRD results of these catalyst samples.
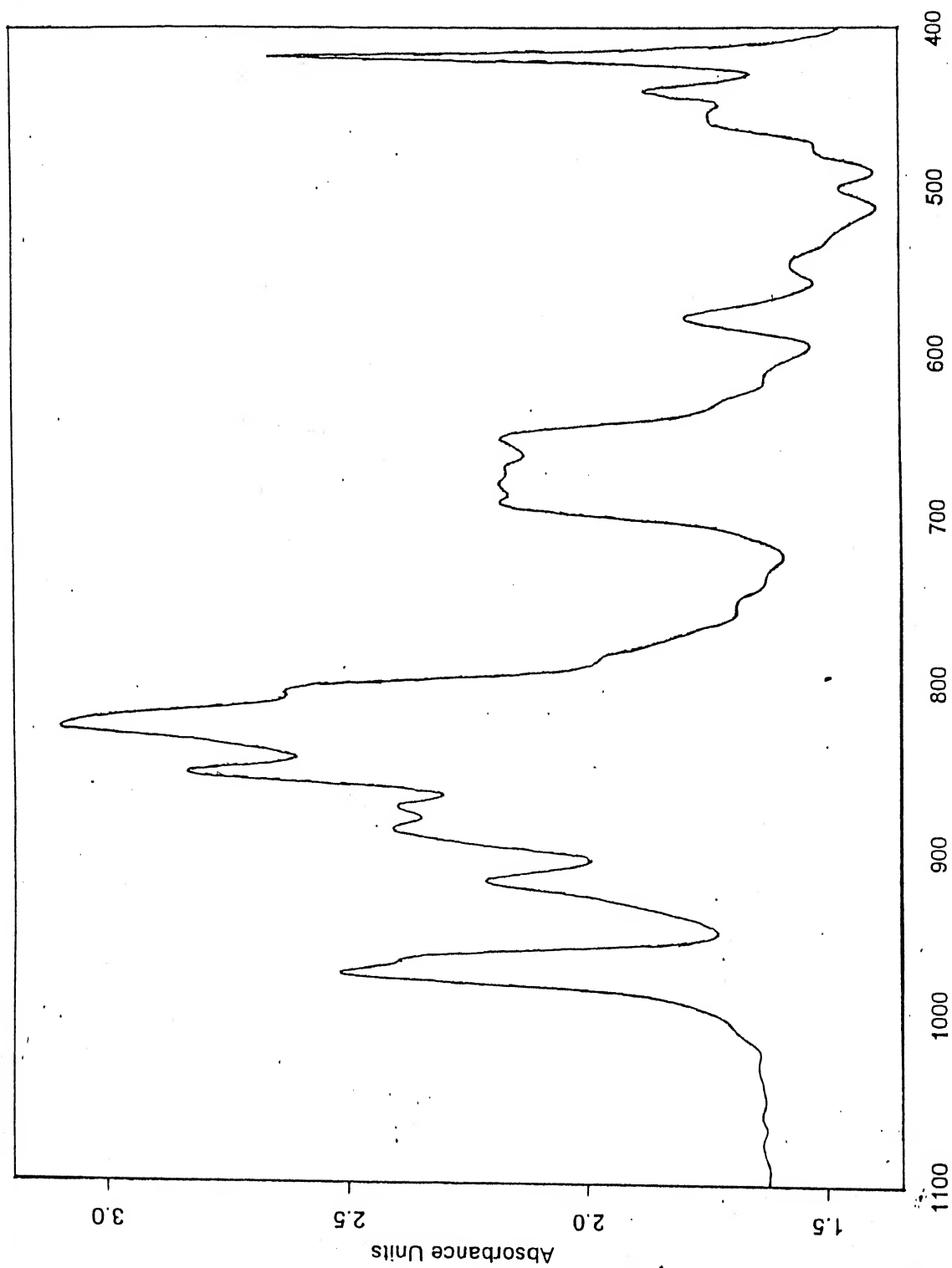
Figure 4.1 FT-IR spectra of $V_2Mg_2O_x$ catalyst

Absorbance Units

30A
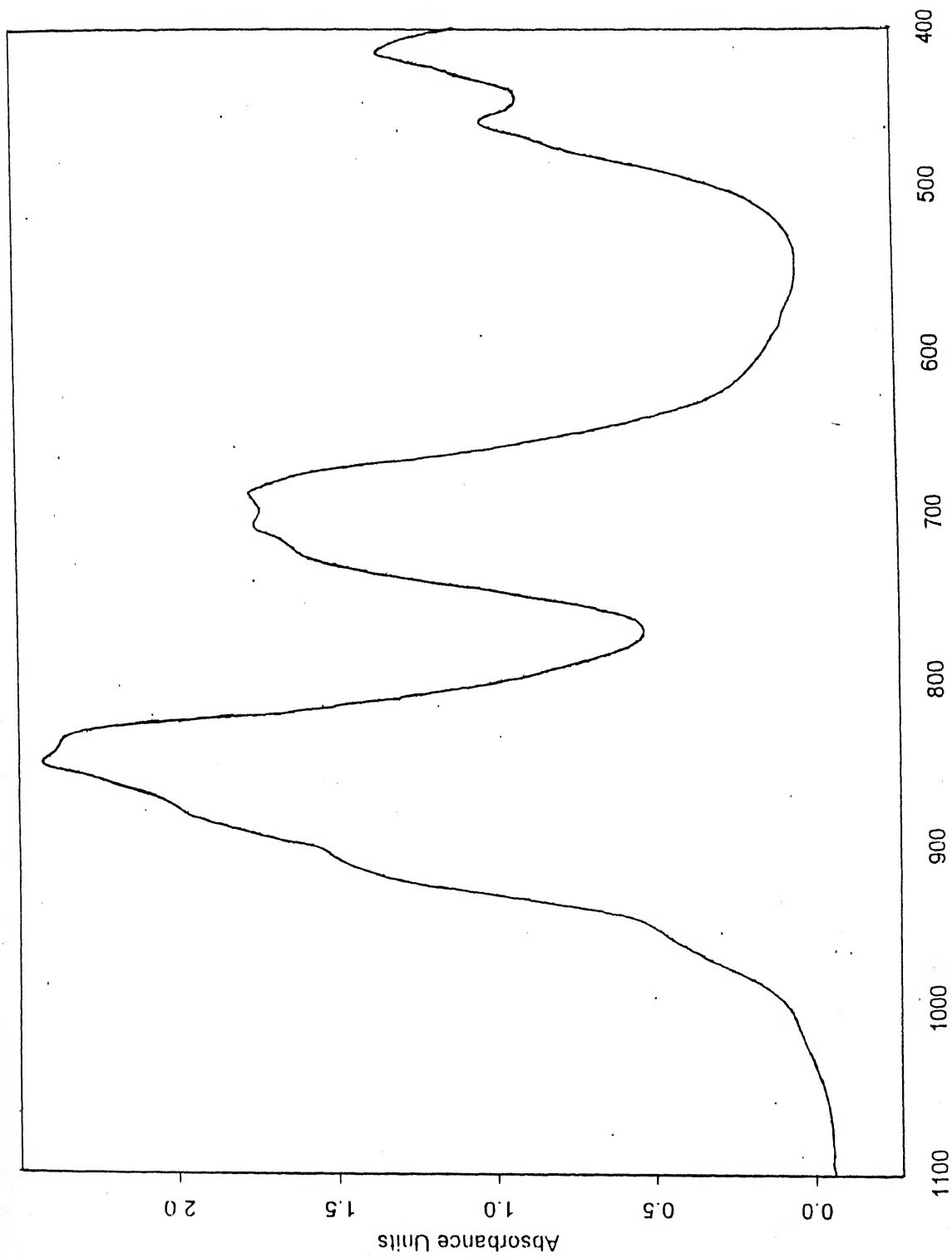
Figure 4.2 FT-IR spectra of $V_2Mg_3O_x$ catalyst
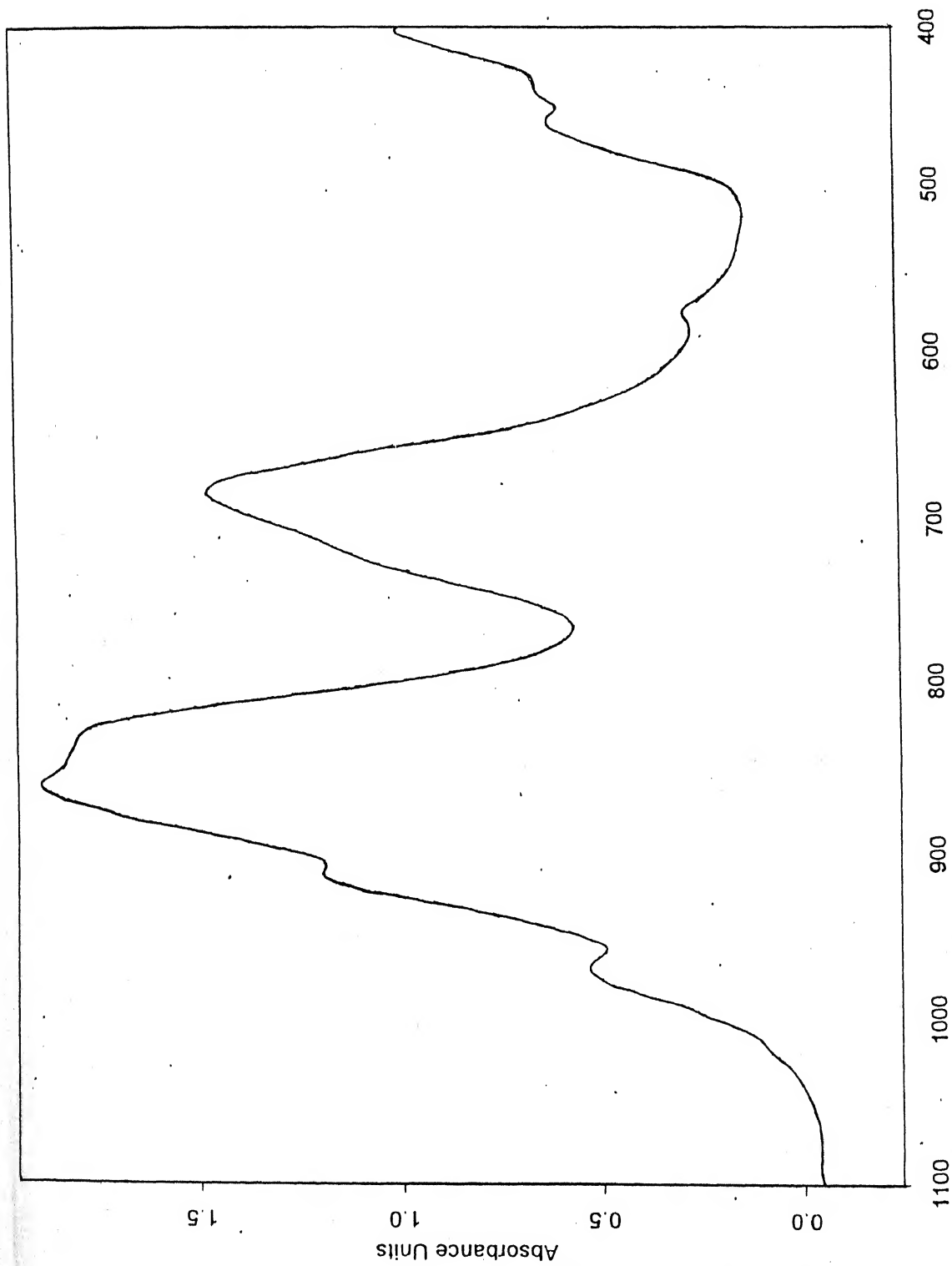
Figure 4.3 FT-IR spectra of V₄Mg₅Oₓ catalyst
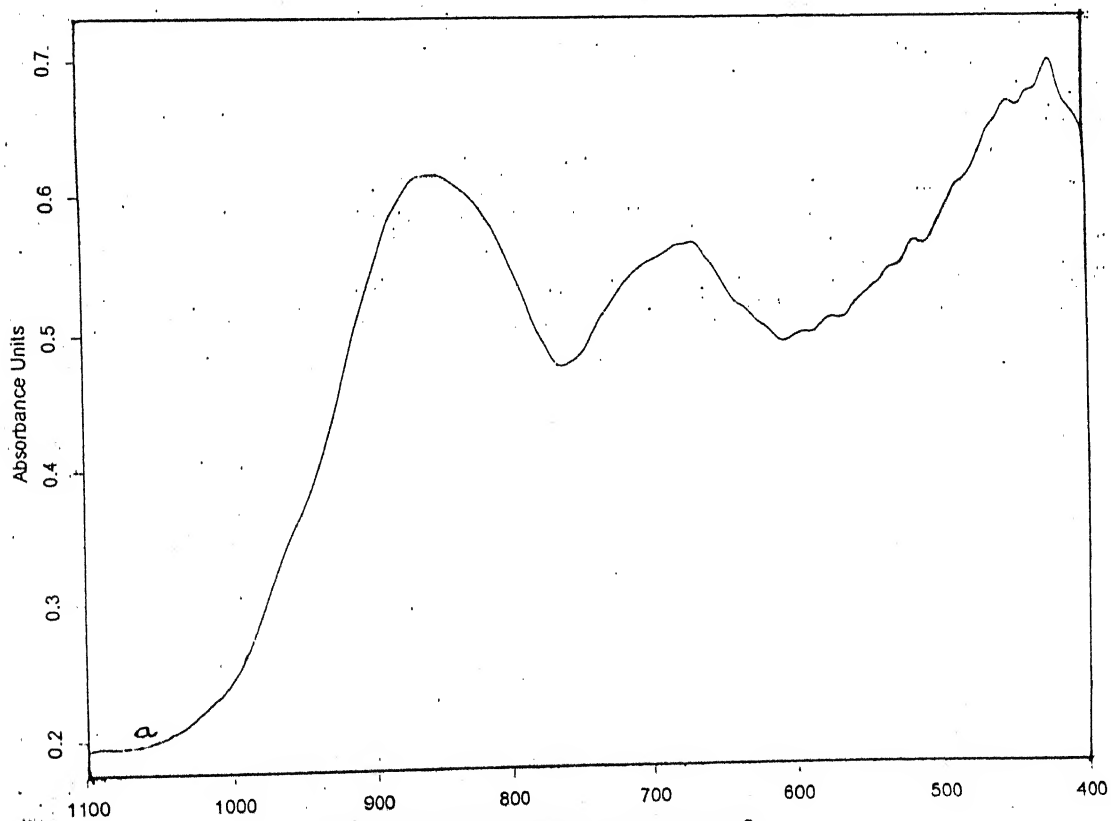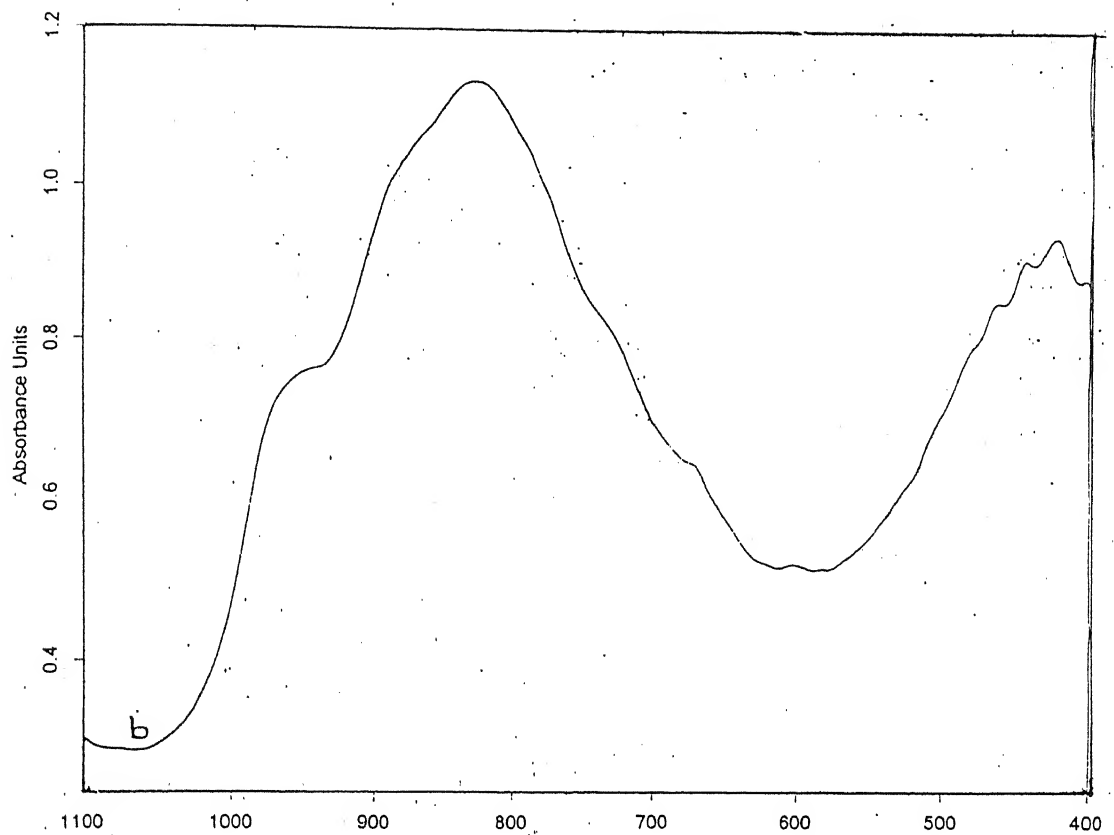
Figure 4.4 FT-IR spectra of

a) $V_1Mg_4O_x$ and b) $Mo_{1.0}V_1Mg_4O_x$
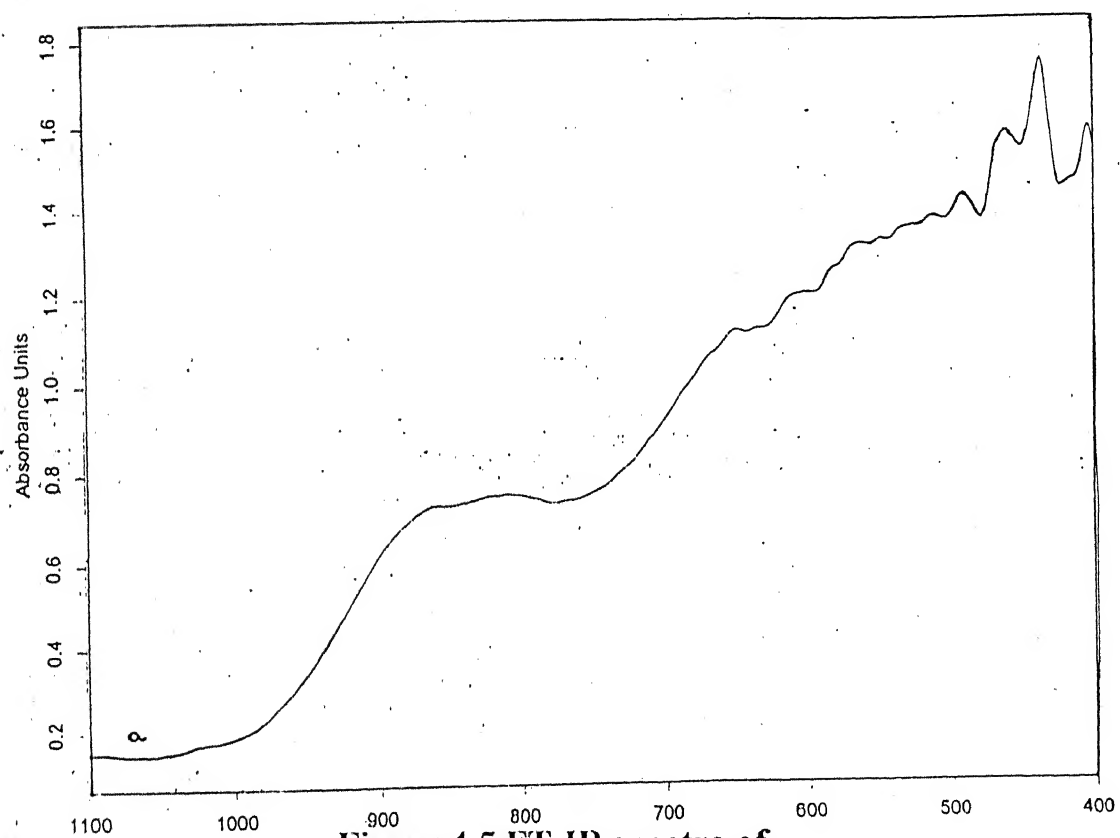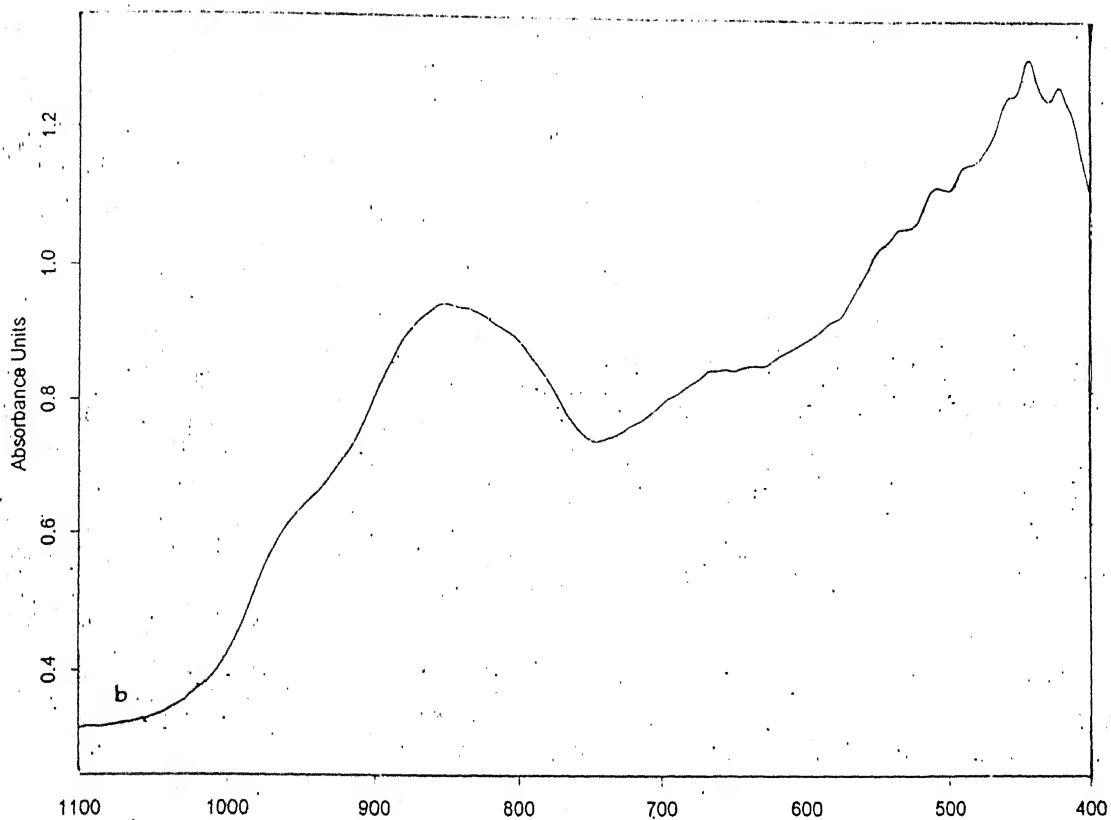
Figure 4.5 FT-IR spectra of

a) $V_1Mg_9O_x$ and b) $Mo_{1.0}V_1Mg_9O_x$

4.4. Temperature Programmed Reduction

The redox properties of the prepared catalysts were probed by temperature programmed reduction (TPR). The experiments were carried out on a Micrometrics 2900 using thermal conductivity detector (TCD) and equipped with online data station. 100 mg of the catalyst sample was taken in a U tube and heated up to 350 ^{0}C in an inert atmosphere to remove any traces of moisture present in the catalyst. Nitrogen (99.5% purity) gas was used as the inert gas. Then, the catalyst was reduced by passing a gas mixture consisting of 5% H_2 in argon. The reduction was studied in the temperature range of 200-800 ^{0}C. The heating rate of the sample was 10 ^{0}C/min.

The TPR results of $V_1Mg_4O_x$ and $Mo_yV_1Mg_4O_x$ catalysts are shown in Figure 4.6. As can be seen from the Figure 4.6, the TPR of the binary V-Mg-O catalyst showed only one peak at a temperature of 650 ^{0}C. The peak started at 500 ^{0}C and reached a maximum at 650 ^{0}C. This temperature was quite high when compared to the reduction temperature of V-Mg-O reported in the literature [17, 21, 24]. In most of the literature 575 ^{0}C was reported as the reduction temperature of V-Mg-O catalysts prepared by impregnation method. One possible reason for the increase in the reduction temperature could be the method of preparation of catalyst. No TPR studies were available in the literature for the V-Mg-O catalysts prepared by citrate method.

In the case of ternary catalysts $Mo_yV_1Mg_4O_x$, one more peak was observed at a temperature of 770 ^{0}C. With an increase in the molybdenum content, the first peak at 650 ^{0}C was shifted to higher temperatures and the intensity of the second peak increased. For instance, for $Mo_yV_1Mg_4O_x$ catalyst the first peak appeared at 730 ^{0}C instead of at 650 ^{0}C. Dejoz [24] et al. reported two extra peaks at 685 ^{0}C and 780 ^{0}C for the Mo-doped V-Mo-Mg-O catalysts.

Similar results were obtained in TPR studies of the $MoyV_1Mg_9O_x$ catalysts. The first peak due to the reduction of vanadium species was obtained at approximately 650 ^0C and the peak due to the reduction of molybdenum species was obtained at around 780 ^0C.
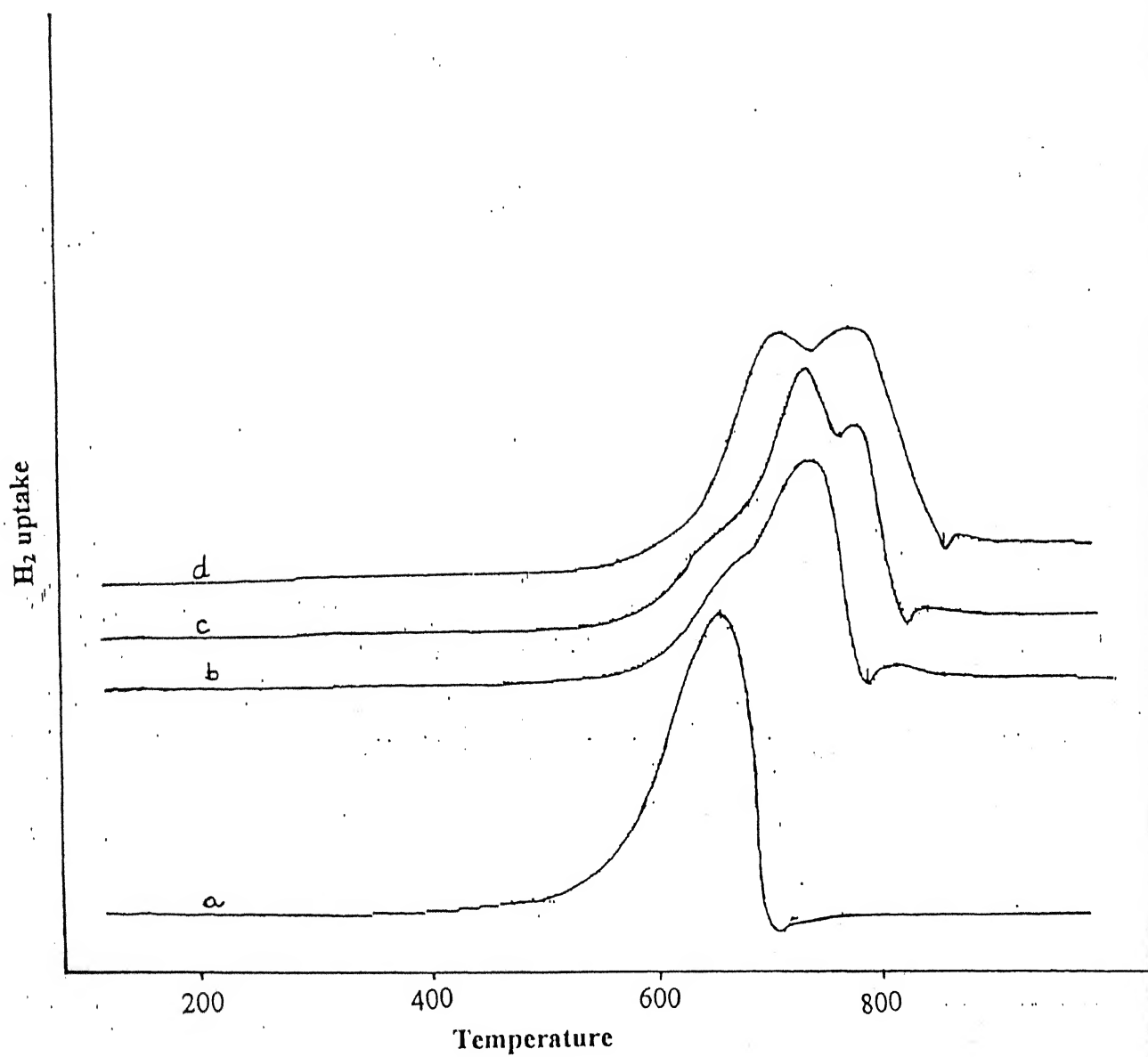
Figure 4.6 TPR analysis of $Mo_yV_1Mg_4O_x$ catalysts
a) $V_1Mg_4O_x$ b) $Mo_{0.1}V_1Mg_4O_x$ c) $Mo_{0.3}V_1Mg_4O_x$ d) $Mo_{1.0}V_1Mg_4O_x$

Results and Discussion

5.1. Reaction conditions

All the runs were carried out in a tubular quartz reactor under constant propane partial pressure. The composition of the feed was 4 mol% propane, 8 mol% oxygen and the rest (88 mol%) nitrogen. Propane and oxygen were used without any purification. Nitrogen was first passed through pyragallol solution and then through silica gel to remove any traces of oxygen and moisture in the gas.

Preliminary runs were conducted to check the contribution of homogeneous reaction and the inertness of quartz particles. In checking the contribution of the homogeneous reaction the volume in the reactor normally filled by the catalyst bed was filled with quartz wool. In checking the effect of quartz particles the normal catalyst bed volume was filled entirely with quartz particles. The other reaction conditions were the same as those for the standard conditions in an ODH reaction. In both the runs a conversion of less than 0.5% was observed at 550 ^{0}C and even less at lower temperatures. Thus the contribution of homogeneous reaction and the effect of quartz particles was not accounted in the ODH of propane.

The significance of external mass transfer effects was studied by measuring the conversion and selectivity at constant W/F_{A0} for different total flow rates in the range of 50-150 ml/min. No mass transfer effects were observed in this range of flow rates. The total flow rate of the feed or the weight of the catalyst was varied to obtain different W/F_{A0} (gcat-h/mol of propane) for the various catalysts investigated. The mass of the catalyst was varied from 0.1 to 0.4 g and the total flow rate was varied from 50 to

150ml/min. All the runs were carried out in the temperature range of 500-550 ^{0}C, specifically at 500, 525 and 550 ^{0}C.

For all the catalytic runs, the major products obtained were propene, carbon monoxide and carbon dioxide. Ethylene and acetylene were detected in minor amounts. For some runs ethane and methane were also observed at 550 ^{0}C. In the present study, the activity and selectivity of the catalyst were defined as

$$\text{Conversion (\%)} = \frac{\text{moles of carbon in products}}{\text{total moles of carbon in exit gases}} \times 100$$

$$\text{Selectivity to product 'X' (\%)} = \frac{\text{moles of carbon in product 'X'}}{\text{total moles of carbon in products}} \times 100$$

$$\text{Carbon balance (\%)} = \frac{\text{total carbon in - total carbon out}}{\text{total carbon in}} \times 100$$

For all the runs reported in the present study, the carbon balance was within the range of 95 to 100%.

5.2. Results

5.2.1. V-Mg-O catalysts

For all the binary catalysts, the runs were carried out at a constant W/F_{A0} and at three different temperatures. The weight of the catalyst used was 0.2 g and the total flow rate of the feed was 100 ml/min. Table 5.1 shows the results of the catalytic runs performed on the binary V-Mg-O catalytic system. For all the catalysts, conversion of propane increased with increasing temperature. The selectivity to propylene decreased with increasing conversion for all the catalysts except for $V_1Mg_9O_x$ catalyst. This decreasing trend was in good agreement with the other published literature on V-Mg-O

system [4, 5, 7, 9, 10]. The reason for the increase of selectivity in the case of $V_1Mg_9O_x$ system can be explained to the lack of sufficient oxygen at 550 ^{0}C (refer to run no. B27 and B29 in Table 5.1).

As can be seen from Table 5.1, the binary catalysts with lower vanadium loading showed high activity in the ODH of propane. The catalysts with higher vanadia content were less active. At 550 ^{0}C and at a W/F$_{A0}$ of 20.4 gcat-h/mol of propane, $V_2Mg_2O_x$ ($Mg_2V_2O_7$) with a vanadia content of about 70 wt% showed a conversion of only 12%, whereas $V_1Mg_9O_x$ showed a conversion of about 55%. Mamedov et al. [5] in their review paper found that highest conversion of propane was obtained at a vanadia loading of approximately 20 wt%. As can be seen from Table 5.2 the catalytic activity and selectivity obtained in the present study on $V_1Mg_4O_x$ and $V_1Mg_9O_x$ are in good agreement with the data obtained by Gao et al. [10].

Though the activity of the catalysts with lower vanadia content was high their selectivity to propene was lower. Of the two catalysts, $V_1Mg_4O_x$ and $V_1Mg_9O_x$, the former showed a higher selectivity to propene. Thus, both $V_1Mg_9O_x$ and $V_1Mg_4O_x$ were selected for further study of doping with molybdenum.

Table 5.1: Conversion and product distribution during ODH of propane on binary catalysts at constant W/F_{A0}

$W/F_{A0} = 20.4$ gcat-h/mol of propane

Catalyst: $V_2Mg_2O_x$ ($Mg_2V_2O_7$)

Run	Temp.	Conv. (%)		Selectivity (%)					
No.	K	C_3H_8	O_2	C_3H_6	CO	CO_2	C_2H_4	CH_4	C_2H_2
B1	773	4.7	3.1	68.6	20.5	10.9	tr	-	-
B2		5.4	3.4	68.2	20.6	11.2	tr	-	-
B3	798	8.7	6.7	66.9	20.7	12.4	tr	-	-
B4		8.0	7.0	65.3	22.1	12.6	tr	-	-
B5	823	12.1	10.1	61.9	22.8	15.3	tr	-	-
B6		12.1	10.5	61.2	23.5	15.3	tr	-	-

tr: Trace

Catalyst: $V_2Mg_3O_x$ ($Mg_3V_2O_8$)

Run	Temp.	Conv. (%)		Selectivity (%)					
No.	K	C_3H_8	O_2	C_3H_6	CO	CO_2	C_2H_4	CH_4	C_2H_2
B7	773	5.3	4.5	49.6	17.7	33.7	tr	-	-
B8		4.9	4.3	53.0	16.8	30.2	tr	-	-
B9	798	7.5	5.4	51.9	17.6	30.5	tr	-	-
B10		7.1	5.3	54.6	17.7	27.7	tr	-	-
B11	823	11.0	8.5	58.4	17.8	23.8	tr	-	-
B12		11.3	8.1	57.6	18.3	24.1	tr	-	-

tr: Trace

Table 5.1 (Contd.)

Catalyst: $V_4Mg_5O_x$

Run	Temp.	Conv. (%)		Selectivity (%)					
No.	K	C_3H_8	O_2	C_3H_6	CO	CO_2	C_2H_4	CH_4	C_2H_2
B13	773	6.4	4.3	61.8	18.4	19.8	tr	-	-
B14		6.0	4.1	59.9	19.5	20.6	tr	-	-
B15	798	7.1	6.0	59.4	17.7	22.9	tr	-	-
B16		7.0	6.3	58.2	18.3	23.5	tr	-	-
B17	823	10.1	8.5	55.6	18.9	25.5	tr	-	-
B18		10.5	8.9	55.0	19.5	25.5	tr	-	-

tr: Trace

Catalyst: $V_1Mg_4O_x$

Run	Temp.	Conv. (%)		Selectivity (%)					
No.	K	C_3H_8	O_2	C_3H_6	CO	CO_2	C_2H_4	CH_4	C_2H_2
B19	773	12.1	17.2	43.9	17.9	38.2	tr	-	-
B20		13.1	28.8	42.5	17.6	39.9	tr	-	-
B21	798	27.5	38.1	41.4	16.9	41.7	tr	-	-
B22		29.1	40.8	42.9	17.4	39.7	tr	-	-
B23	823	45.1	76.8	33.7	21.8	44.1	0.4	tr	tr
B24		46.1	77.1	35.4	21.5	42.8	0.3	tr	tr

tr: Trace

Table 5.1 (Cont.)

Catalyst: $V_1Mg_9O_x$

Run	Temp.	Conv. (%)		Selectivity (%)					
No.	K	C_3H_8	O_2	C_3H_6	CO	CO_2	C_2H_4	CH_4	C_2H_2
B25	773	17.9	25.5	37.3	16.1	46.6	tr	-	-
B26		18.4	28.5	38.1	16.3	45.6	tr	-	-
B27	798	47.6	91.8	27.9	17.8	54.0	0.3	-	-
B28	–	47.0	89.9	29.7	17.7	52.3	0.3	-	-
B29	823	55.0	100	31.4	20.8	47.3	0.5	tr	tr
B30		55.1	100	32.1	21.4	46.1	0.4	tr	tr

tr: Trace

Table 5.2: Comparison of present study with literature

Catalyst used	Present study		Gao et al. [10]	
	Conversion of propane	Selectivity to propene	Conversion of propane	Selectivity to propene
$V_1Mg_4O_x$	55.0	31.4	53.2	30.3
$V_1Mg_9O_x$	46.1	35.4	46.0	35.7

$W/F_{A0} = 20.4$ gcat-h/mol of propane

Temperature: 550 ^{0}C

5.2.2. Mo-V-Mg-O catalysts

5.2.2.1. Effect of Molybdenum

For all the ternary Mo-V-Mg-O catalysts, runs were conducted at the same conditions as used for the binary catalysts for studying the effect of molybdenum on binary catalysts. Table 5.3 shows the conversion and selectivity obtained on the molybdenum doped $Mo_{0.1}V_1Mg_4O_x$ and $Mo_{0.3}V_1Mg_4O_x$ systems at a constant W/F_{A0} (20.4 gcat-h/mol of propane) and at different temperatures. Table 5.4 shows the conversion and selectivity for Mo doped $Mo_yV_1Mg_9O_x$ system under similar conditions.

As can be observed from the Tables 5.3 and 5.4, the selectivity of the binary catalysts improved with molybdenum doping. A gradual increase in selectivity was observed with increasing Mo content. It was also noticed that the activity of the catalysts decreased gradually with increasing Mo content. Very low conversions (<5%) were obtained on $Mo_yV_1Mg_4O_x$ catalysts having Mo/V atomic ratio above 0.3. Of the two binary systems doped with molybdenum, $Mo_yV_1Mg_9O_x$ catalysts were found to be better as these showed a higher activity for the same amount of Mo loading. Thus, $Mo_yV_1Mg_9O_x$ system was selected for a detailed study.

Table 5.3. : Conversion and product distribution during ODH of propane on $Mo_yV_1Mg_4O_x$ system at constant W/F_{A0}

W/F_{A0} = 20.4 gcat-h/mol of propane

Catalyst: $Mo_{0.1}V_1Mg_4O_x$

Run	Temp.	Conv. (%)		Selectivity (%)					
No.	K	C_3H_8	O_2	C_3H_6	CO	CO_2	C_2H_4	CH_4	C_2H_2
T1	773	5.7	4.8	67.6	8.8	23.6	tr	-	-
T2		6.7	5.1	66.5	9.1	24.4	tr	-	-
T3	798	13.1	10.2	63.7	16.6	19.7	tr	-	-
T4		12.9	9.8	63.9	16.3	19.8	tr	-	-
T5	823	21.7	17.5	62.8	16.9	20.3	tr	-	-
T6		20.5	16.9	63.3	16.8	19.9	tr	-	-

tr: trace

Catalyst: $Mo_{0.3}V_1Mg_4O_x$

Run	Temp.	Conv. (%)		Selectivity (%)					
No.	K	C_3H_8	O_2	C_3H_6	CO	CO_2	C_2H_4	CH_4	C_2H_2
T7	773	2.4	1.8	78.6	11.7	9.7	tr	-	-
T8		2.5	1.9	78.2	12.4	10.4	tr	-	-
T9	798	4.7	3.5	76.7	13.3	10.0	tr	-	-
T10		4.8	3.9	77.2	12.5	10.3	tr	-	-
T11	823	10.8	8.9	74.2	12.8	12.9	tr	-	-
T12		10.1	9.2	74.6	12.3	13.1	tr	-	-

tr: trace

Table 5.4. : Conversion and product distribution during ODH of propane on $Mo_yV_1Mg_9O_x$ system at constant W/F_{A0}

W/F_{A0} =20.4 gcat-h/mol of propane

Catalyst: $Mo_{0.1}V_1Mg_9O_x$

Run	Temp.	Conv. (%)		Selectivity (%)					
No.	K	C_3H_8	O_2	C_3H_6	CO	CO_2	C_2H_4	CH_4	C_2H_2
T13	773	11.2	17.6	53.3	10.2	36.4	tr	-	-
T14		12.0	18.2	51.7	11.1	37.2	tr	-	-
T15	798	26.9	44.9	45.4	16.8	37.8	tr	-	-
T16		26.3	40.8	46.5	16.5	37.0	tr	-	-
T17	823	48.2	89.6	35.5	22.5	41.7	0.3	tr	tr
T18		43.6	71.9	41.3	21.3	36.9	0.4	tr	tr

tr: trace

Catalyst: $Mo_{0.3}V_1Mg_9O_x$

Run	Temp.	Conv. (%)		Selectivity (%)					
No.	K	C_3H_8	O_2	C_3H_6	CO	CO_2	C_2H_4	CH_4	C_2H_2
T19	773	10.08	13.6	59.6	13.9	26.5	tr	-	-
T20		10.57	14.2	60.2	14.4	25.4	tr	-	-
T21	798	22.6	32.4	57.1	15.5	27.4	tr	-	-
T22		22.1	31.0	58.2	15.2	26.6	tr	-	-
T23	823	40.6	68.4	46.8	21.9	30.9	0.3	tr	tr
T24		36.0	55.9	52.3	19.6	27.7	0.4	tr	tr

tr: trace

Table 5.4 (Contd.)

Catalyst: $Mo_{0.6}V_1Mg_9O_x$

Run	Temp.	Conv. (%)		Selectivity (%)					
No.	K	C_3H_8	O_2	C_3H_6	CO	CO_2	C_2H_4	CH_4	C_2H_2
T25	773	5.7	4.8	75.6	8.8	15.6	-	-	-
T26		5.4	5.1	74.7	9.3	16.0	-	-	-
T27	798	10.7	9.6	73.7	12.9	13.4	-	-	-
T28		10.6	9.5	73.0	13.3	13.7	-	-	-
T29	823	19.0	16.7	71.9	13.4	14.7	tr	-	-
T30		18.3	16.1	72.1	13.2	14.7	tr	-	-

tr: trace

Catalyst: $Mo_{1.0}V_1Mg_9O_x$

Run	Temp.	Conv. (%)		Selectivity (%)					
No.	K	C_3H_8	O_2	C_3H_6	CO	CO_2	C_2H_4	CH_4	C_2H_2
T31	773	2.9	1.8	79.8	8.9	11.3	-	-	-
T32		2.8	2.1	80.4	8.3	11.3	-	-	-
T33	798	5.9	4.5	77.3	13.2	9.4	-	-	-
T34		6.4	5.3	76.9	13.5	9.6	-	-	-
T35	823	10.5	8.9	74.1	19.4	6.5	-	-	-
T36		10.5	9.2	74.3	19.4	6.2	-	-	-

tr: trace

5.2.2.2. Effect of W/F$_{A0}$ and Mo loading on conversion and selectivity

The effect of W/F$_{A0}$ on the activity and selectivity of the different Mo$_y$V$_1$Mg$_9$O$_x$ catalysts was investigated at 550 ^{0}C. W/F$_{A0}$ was varied in the range of 6.8 to 81.6 gcat-hr/mol of propane by varying the mass of the catalyst in the range of 0.1-0.4 g and/or the total flow rate in the range of 50-150 ml/min. For all the runs, the inlet mole fraction of C$_3$H$_8$, O$_2$ and N$_2$ were 0.04, 0.08 and 0.88 respectively. Figure 5.1 shows the effect of W/F$_{A0}$ on propane conversion at 550 ^{0}C for the Mo$_y$V$_1$Mg$_9$O$_x$ catalysts as well as the undoped V$_1$Mg$_9$O$_x$ catalyst, whereas the detailed product distribution for these runs is given in Table5.5.

As can be seen from Figure 5.1, with increasing Mo content of the catalyst, the activity decreased significantly. For instance, a conversion of only 26.0% was obtained on Mo$_{1.0}$V$_1$Mg$_9$O$_x$ catalyst, whereas a conversion of 58.8% was obtained on V$_1$Mg$_9$O$_x$ at the same temperature and W/F$_{A0}$. The initial rate of reaction of propane, calculated from the initial slope of the Figure 5.1, decreased from 0.042 gmol/h-gcat for V$_1$Mg$_9$O$_x$ catalyst to 0.0047 gmol/h-gcat for Mo$_{1.0}$V$_1$Mg$_9$O$_x$ catalyst. Thus the activation energy in the partial oxidation of propane on Mo-doped catalysts could be modified by the incorporation of the Mo ions. If the lattice oxygen is involved in the ODH reactions, then the catalyst reducibility can modify the rata of alkane activation and the rate of the selective oxidation. As discussed in Section 4.4, TPR studies showed that the temperature of maximum reduction increased with an increase in the Mo content of the catalyst.

The variation of selectivity of propene with propane conversion for the different catalysts at a constant temperature of 550 ^{0}C is shown in Figure 5.2. For all the catalysts, the selectivity of propene decreased with increasing propane conversion. At a fixed conversion, the selectivity to propene increased with increasing Mo content up to Mo/V atomic ratio of 0.6. Further increase in the Mo/V atomic ratio did not have a significant effect on the selectivity of the catalyst.

The effect of Mo/V atomic ratio on the selectivities of C_3H_6, CO and CO_2 at a conversion of 30% is shown in Figure 5.3. As can be seen from the Figure 5.3, the selectivity of CO was not significantly affected by doping Mo and the increase in selectivity of propene was mostly due to the decrease in the selectivity of CO_2. Thus, the formation of CO_2, rather than CO, is influenced by the catalyst composition.

Several investigators have postulated reaction pathways for the ODH of propane [18, 26, 27]. The first step is most likely the activation of C-H bond of propane to give an adsorbed C_3H_7, which subsequently converts to C_3H_6 on the surface. The C_3H_6 can desorb into the gas phase or be further oxygenated to CO and CO_2. Possibly a small amount of propane can also be converted to CO_2 by a parallel route. The possible reactions can be represented as

$$C_3H_8 \xrightarrow{\;k_1\;} C_3H_6 \xrightarrow{\;k_4\;} CO$$
$$C_3H_8 \xrightarrow{\;k_2\;} CO_2 \qquad C_3H_6 \xrightarrow{\;k_3\;} CO_2$$
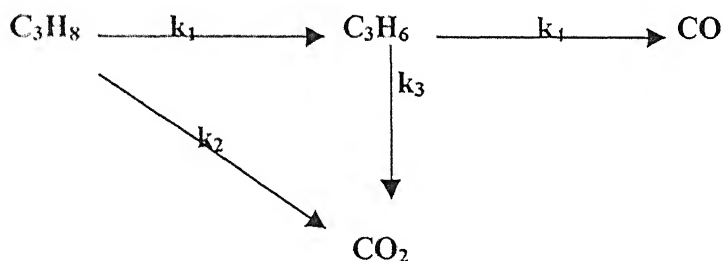
Experimental evidence indicates that for V-Mg-O catalysts, the direct formation of CO_2 from propane is not appreciable. For V/Nb/Ti and V_2O_5/Nb_2O_5 catalysts, the direct formation of CO_2 from propane was negligible [27]. The variation of product selectivities with Mo/V atomic ratio suggests that the sites responsible for the total oxidation are reduced due to the incorporation of Mo. The selectivity of propene will be determined by the ratio of $k_1/(k_3+k_4)$. The activity studies (Figure 5.1) show that k_1 is lower for the Mo containing catalysts, whereas the selectivity results (Figure 5.3) indicate that k_3 is significantly reduced with an increase in Mo loading.
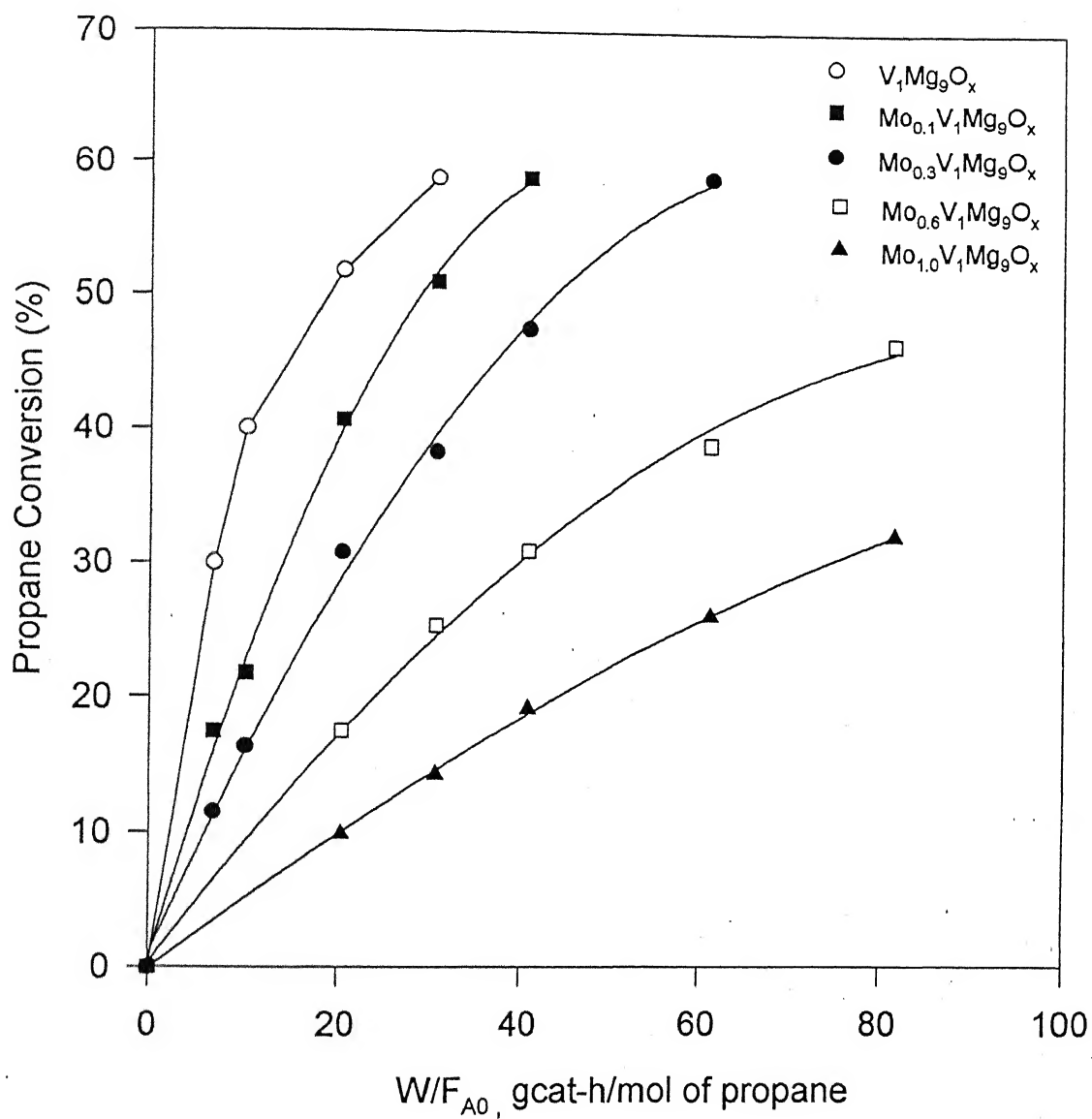
Figure 5.1 Effect of W/F$_{A0}$ on propane conversion on Mo$_y$V$_1$Mg$_9$O$_x$ catalysts at a temperature of 550 ^{0}C

Table 5.5. : Conversion and product distribution during ODH of propane on $Mo_yV_1Mg_9O_x$ system at different W/F_{A0}

Catalyst: $V_1Mg_9O_x$

Run	W/F$_{A0}$	Conv. (%)		Selectivity (%)					
No.	gcat-h/mol	C_3H_8	O_2	C_3H_6	CO	CO_2	C_2H_4	CH_4	C_2H_2
T37	6.8	31.6	46.9	42.0	18.1	39.7	0.2	tr	tr
T38	10.2	42.9	76.7	37.3	22.1	40.2	0.3	tr	tr
T39	20.4	51.8	93.2	33.2	24.7	41.7	0.4	tr	tr
T40	30.6	57.1	100	30.0	27.5	42.0	0.5	tr	tr

tr: trace

Catalyst: $Mo_{0.1}V_1Mg_9O_x$

Run	W/F$_{A0}$	Conv. (%)		Selectivity (%)					
No.	gcat-h/mol	C_3H_8	O_2	C_3H_6	CO	CO_2	C_2H_4	CH_4	C_2H_2
T41	6.8	17.4	18.1	60.2	14.5	25.3	tr	-	-
T42	10.2	21.7	24.5	57.0	16.1	26.8	tr	-	-
T43	20.4	40.6	68.4	46.8	21.4	31.5	0.3	-	-
T44	30.6	50.9	78.6	37.5	26.4	35.9	0.2	tr	tr
T45	40.8	58.8	96.8	31.9	30.5	37.1	0.5	tr	tr

tr: trace

Table 5.5 (Contd.)

Catalyst: $Mo_{0.3}V_1Mg_9O_x$

Run	W/F$_{A0}$	Conv. (%)		Selectivity (%)					
No.	gcat-h/mol	C$_3$H$_8$	O$_2$	C$_3$H$_6$	CO	CO$_2$	C$_2$H$_4$	CH$_4$	C$_2$H$_2$
T46	6.8	11.5	10.8	68.8	11.5	19.7	-	-	-
T47	10.2	16.3	17.2	62.2	13.7	24.0	-	-	-
T48	20.4	30.8	42.2	53.0	18.4	28.5	tr	tr	tr
T59	30.6	38.3	61.4	48.3	21.4	30.2	tr	tr	tr
T50	40.8	47.5	75.4	41.5	24.3	33.9	0.3	tr	tr
T51	61.2	58.8	95.3	34.2	27.4	37.9	0.4	tr	tr

tr: trace

Catalyst: $Mo_{0.6}V_1Mg_9O_x$

Run	W/F$_{A0}$	Conv. (%)		Selectivity (%)					
No.	gcat-h/mol	C$_3$H$_8$	O$_2$	C$_3$H$_6$	CO	CO$_2$	C$_2$H$_4$	CH$_4$	C$_2$H$_2$
T52	20.4	17.4	15.5	72.8	13.2	14.0	tr	-	-
T53	30.6	25.3	28.65	60.7	17.4	21.9	tr	-	-
T54	40.8	30.9	38.9	56.2	20.3	23.4	tr	-	-
T55	61.2	37.9	51.8	46.1	23.8	29.6	0.5	tr	tr
T56	81.6	46.4	69.9	40.4	27.2	31.8	0.6	tr	tr

tr: trace

Table 5.5 (Contd.)

Catalyst: $Mo_{1.0}V_1Mg_9O_x$

Run No.	W/F$_{A0}$ gcat-h/mol	Conv. (%)		Selectivity (%)					
		C_3H_8	O_2	C_3H_6	CO	CO_2	C_2H_4	CH_4	C_2H_2
T57	20.4	9.9	8.4	79.8	12.3	7.9	-	-	-
T58	30.6	14.3	12.2	75.3	13.6	11.0	-	-	-
T59	40.8	19.2	20.8	69.4	15.9	14.6	-	-	-
T60	61.2	25.1	32.7	61.7	19.6	18.7	tr	-	-
T61	81.6	32.1	41.5	54.8	23.0	22.1	tr	-	-

tr: trace
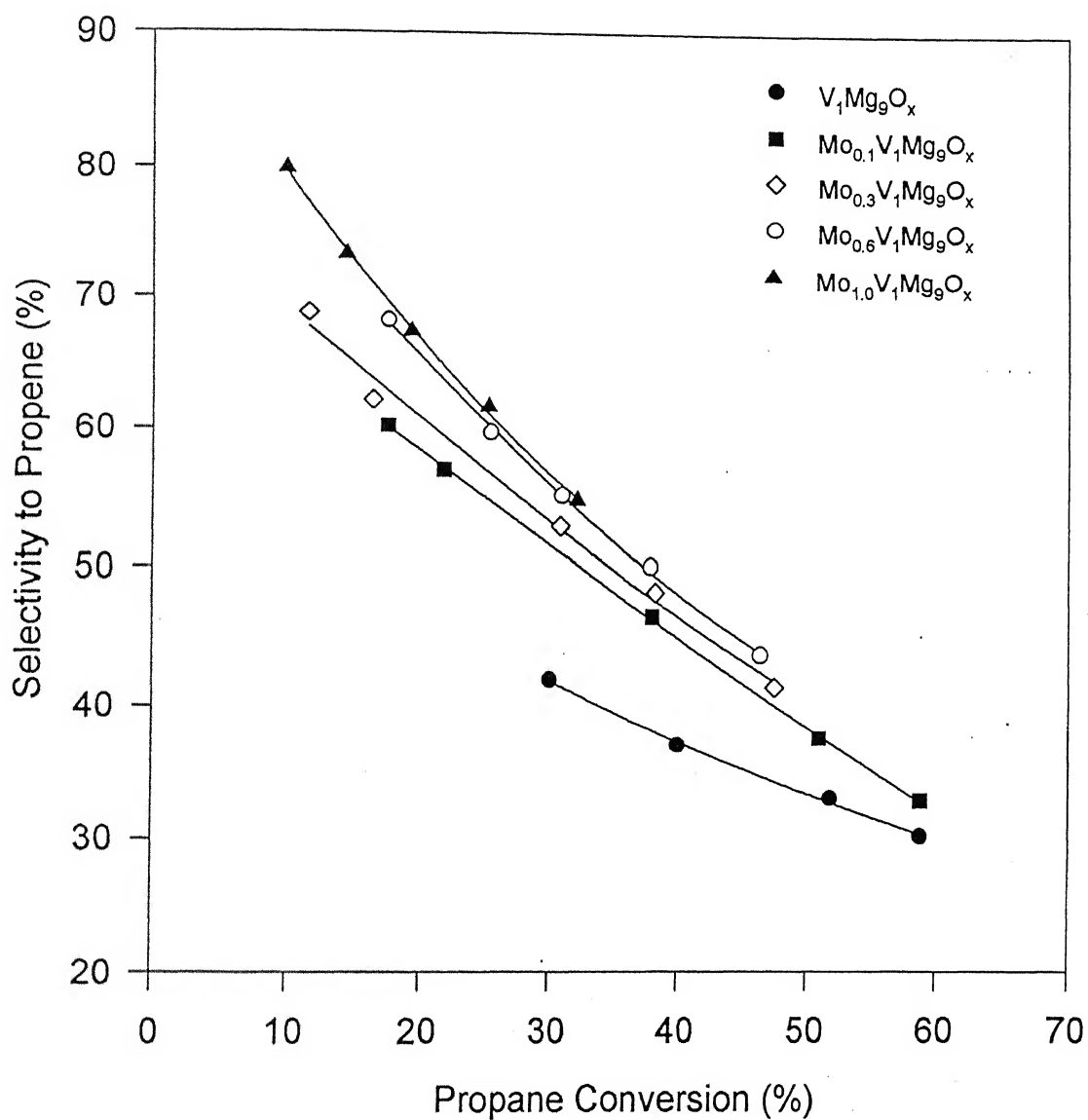
Figure 5.2 Variation of propene selectivity with propane conversion on $Mo_yV_1Mg_9O_x$ catalysts at 550 ^{0}C
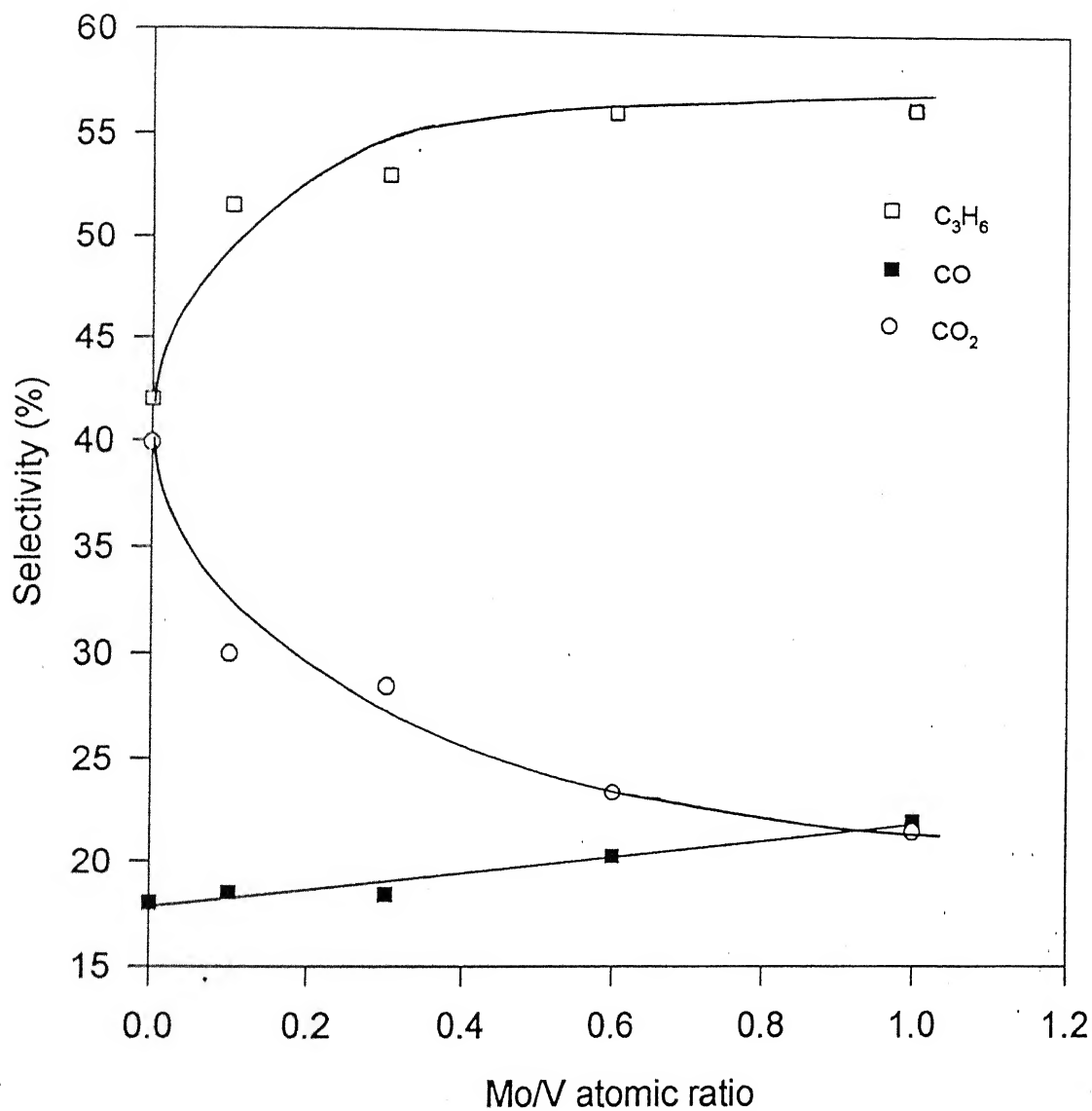
Figure 5.3 Variation of selectivity of products with Mo/V atomic ratio at 30% propane conversion

5.2.2.3. Effect of temperature

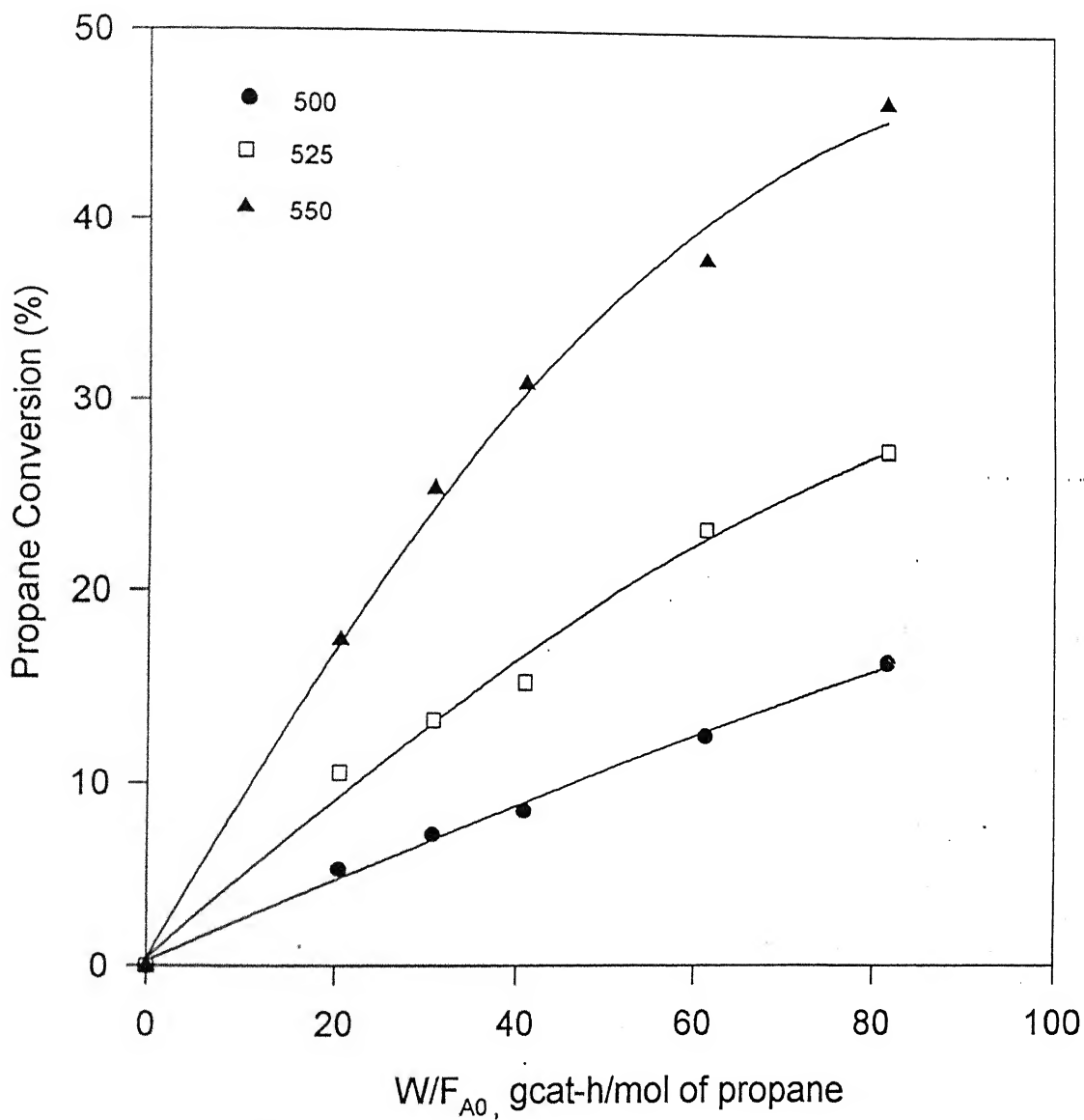The effect of temperature on the conversion and selectivity for $Mo_{0.6}V_1Mg_9O_x$ and $Mo_{0.3}V_1Mg_4O_x$ was also investigated in the temperature range of 500-550 ^{0}C. The effect of W/F_{A0} at the three temperatures for $Mo_{0.6}V_1Mg_9O_x$ is shown in Figure 5.4, whereas the corresponding plots for $Mo_{0.3}V_1Mg_4O_x$ are shown in Figure 5.5. The detailed product distribution at the three different temperatures is given in Table 5.6 and 5.7, respectively. As expected for both the catalysts, the propane conversion increased with temperature. The variation of propene selectivity with propane conversion for the three temperatures is shown in Figure 5.6 and 5.7 for $Mo_{0.6}V_1Mg_9O_x$ and $Mo_{0.3}V_1Mg_4O_x$, respectively. The selectivity to propene also increased with temperature for both the catalysts. For instance, at a propane conversion of 15.0%, the propene selectivity obtained with $Mo_{0.6}V_1Mg_9O_x$ increased from 61% to 76% as the temperature was increased from 500 to 550 ^{0}C. Comparing Figures 5.6 and 5.7, it can be seen that at a given conversion and temperature, the propene selectivity obtained with $Mo_{0.6}V_1Mg_9O_x$ was higher than with $Mo_{0.3}V_1Mg_4O_x$. The data collected in Tables 5.6 and 5.7 shows that the selectivities of CO and CO_2 decreased with increasing temperature for both the catalysts. The effect of temperature was more pronounced on the CO_2 selectivity. For instance, for $Mo_{0.6}V_1Mg_9O_x$ catalyst at 15% conversion, the CO_2 selectivity decreased from 23.2% to 12.0% as the temperature was increased from 500 to 550 ^{0}C. The corresponding change in the CO selectivity was from 15.8% to 12%.

This trend of increasing propene selectivity with increasing temperature shows that the activation energy for the oxidative dehydrogenation reaction is higher than the activation energy for the formation of carbon oxides. In other words, the activation energy for k_1 is higher than the activation energy for k_3 and k_4. Similarly, Dejoz et al. [24] also reported that for the ODH of n-butane on Mo-doped VMgO catalysts, the activation energy for the ODH reactions were higher than that for the formation of carbon oxides.

activation energy for the ODH reactions were higher than that for the formation of carbon oxides.

An estimate of the activation energy for the consumption of propane was made from the initial rates at the three temperatures. The initial rates were calculated from the slope of the conversion vs. W/F_{A0} plots (Figures 5.4 and 5.5) at W/F_{A0} equal to zero. The Arrhenius plots for the two catalysts are shown in Figure 5.8. The activation energies calculated from the slopes of these plots were 123.1 and 158 kJ/mol for $Mo_{0.6}V_1Mg_9O_x$ and $Mo_{0.3}V_1Mg_4O_x$, respectively. No published information is available on the activation energies for ODH of propane on Mo-doped V-Mg-O catalysts. However, these activation energies are in the same range as the value of 140 kJ/mol reported by Patel et al. [33] for V-Mg-O catalysts.

Figure 5.4 Effect of W/F$_{A0}$ on propane conversion at different temperatures on Mo$_{0.6}$V$_1$Mg$_9$O$_x$
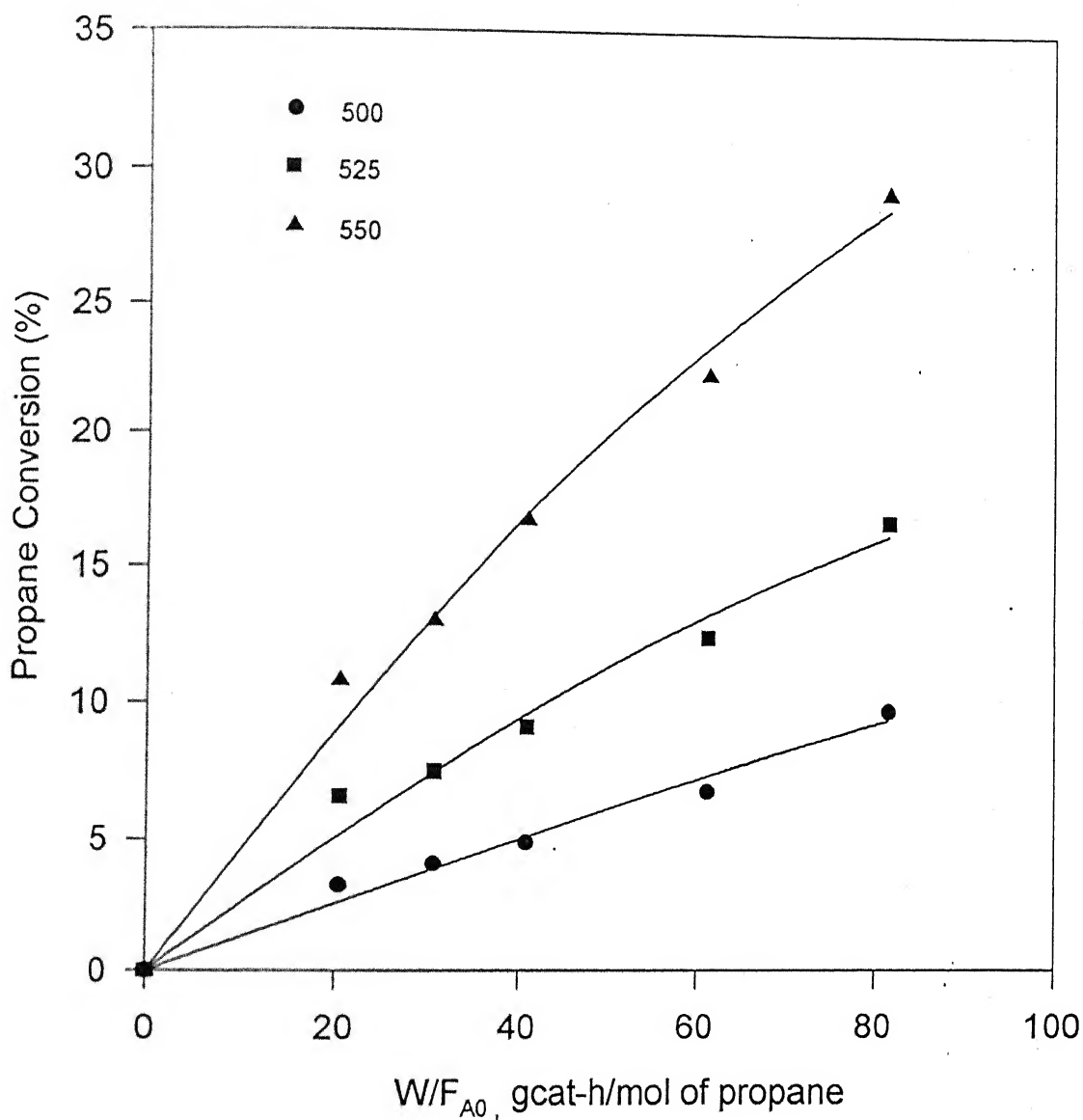
Figure 5.5 Effect of W/F$_{A0}$ on propane conversion for different temperatures on Mo$_{0.3}$V$_1$Mg$_4$O$_x$

Table 5.6. : Conversion and product distribution during ODH of propane on $Mo_{0.6}V_1Mg_9O_x$ system at different temperatures

Temperature: 500 ^{0}C

Run No.	W/F_{A0} gcat-h/mol	Conv. (%)		Selectivity (%)					
		C_3H_8	O_2	C_3H_6	CO	CO_2	C_2H_4	CH_4	C_2H_2
T62	20.4	5.4	6.1	77.5	10.5	12.0	-	-	-
T63	30.6	7.2	9.9	76.1	11.4	12.5	-	-	-
T64	40.8	8.6	14.6	73.2	12.7	14.1	-	-	-
T65	61.2	12.5	15.1	63.6	14.4	21.9	-	-	-
T66	81.6	16.4	25.9	59.2	16.9	23.9	-	-	-

Table 5.6 (Contd.)

Temperature: 525 ^{0}C

Run No.	W/F$_{A0}$ gcat-h/mol	Conv. (%)		Selectivity (%)					
		C$_3$H$_8$	O$_2$	C$_3$H$_6$	CO	CO$_2$	C$_2$H$_4$	CH$_4$	C$_2$H$_2$
T67	20.4	10.6	9.6	74.4	12.2	13.4	-	-	-
T68	30.6	13.3	14.4	70.4	13.5	16.0	-	-	-
T69	40.8	15.3	20.3	68.9	14.7	16.4	-	-	-
T70	61.2	23.3	29.2	55.4	17.9	16.6	tr	-	-
T71	81.6	27.3	40.4	53.6	20.4	26.0	tr	-	-

tr: trace

Temperature: 550 ^{0}C

Run No.	W/F$_{A0}$ gcat-h/mol	Conv. (%)		Selectivity (%)					
		C$_3$H$_8$	O$_2$	C$_3$H$_6$	CO	CO$_2$	C$_2$H$_4$	CH$_4$	C$_2$H$_2$
T72	20.4	17.4	15.8	72.8	13.2	14.0	tr	-	-
T73	30.6	25.3	28.7	60.7	18.2	21.1	tr	-	-
T74	40.8	30.9	38.9	56.2	20.3	23.4	tr	-	-
T75	61.2	37.9	51.8	46.1	23.3	30.1	0.5	tr	tr
T76	81.6	46.4	69.9	40.9	27.2	31.3	0.6	tr	tr

tr: trace

Table 5.7. : Conversion and product distribution during ODH of propane on $Mo_{0.3}V_1Mg_4O_x$ system at different temperatures

Temperature: 500 ^{0}C

Run No.	W/F_{A0} gcat-h/mol	Conv. (%)		Selectivity (%)					
		C_3H_8	O_2	C_3H_6	CO	CO_2	C_2H_4	CH_4	C_2H_2
T77	20.4	2.4	1.7	78.6	11.7	9.7	-	-	-
T78	30.6	3.6	1.9	77.4	12.7	9.9	,-	-	-
T79	40.8	5.2	3.2	75.9	13.5	10.5	-	-	-
T80	61.2	6.8	4.4	71.8	14.5	13.6	-	-	-
T81	81.6	8.7	6.9	63.9	16.8	19.2	-	-	-

Table 5.7 (Contd.)

Temperature: 525 ^{0}C

Run	W/F$_{A0}$	Conv. (%)		Selectivity (%)					
No.	gcat-h/mol	C$_3$H$_8$	O$_2$	C$_3$H$_6$	CO	CO$_2$	C$_2$H$_4$	CH$_4$	C$_2$H$_2$
T82	20.4	4.7	2.3	80.8	7.9	11.3	-	-	-
T83	30.6	7.0	4.9	76.2	11.1	12.7	-	-	-
T84	40.8	9.0	6.8	75.4	13.4	11.1	-	-	-
T85	61.2	12.5	10.9	68.5	16.6	14.9	tr	-	-
T86	81.6	16.6	14.4	63.4	18.9	17.7	tr	-	-

tr: trace

Temperature: 550 ^{0}C

Run	W/F$_{A0}$	Conv. (%)		Selectivity (%)					
No.	gcat-h/mol	C$_3$H$_8$	O$_2$	C$_3$H$_6$	CO	CO$_2$	C$_2$H$_4$	CH$_4$	C$_2$H$_2$
T87	20.4	10.8	8.5	74.2	12.8	12.9	-	-	-
T88	30.6	13.0	9.54	71.4	14.7	13.9	-	-	-
T89	40.8	16.7	10.91	69.8	16.1	14.0	-	-	-
T90	61.2	22.3	22.5	61.8	19.9	18.3	tr	-	-
T91	81.6	29.2	31.0	55.6	23.5	20.9	tr	-	-

tr: trace
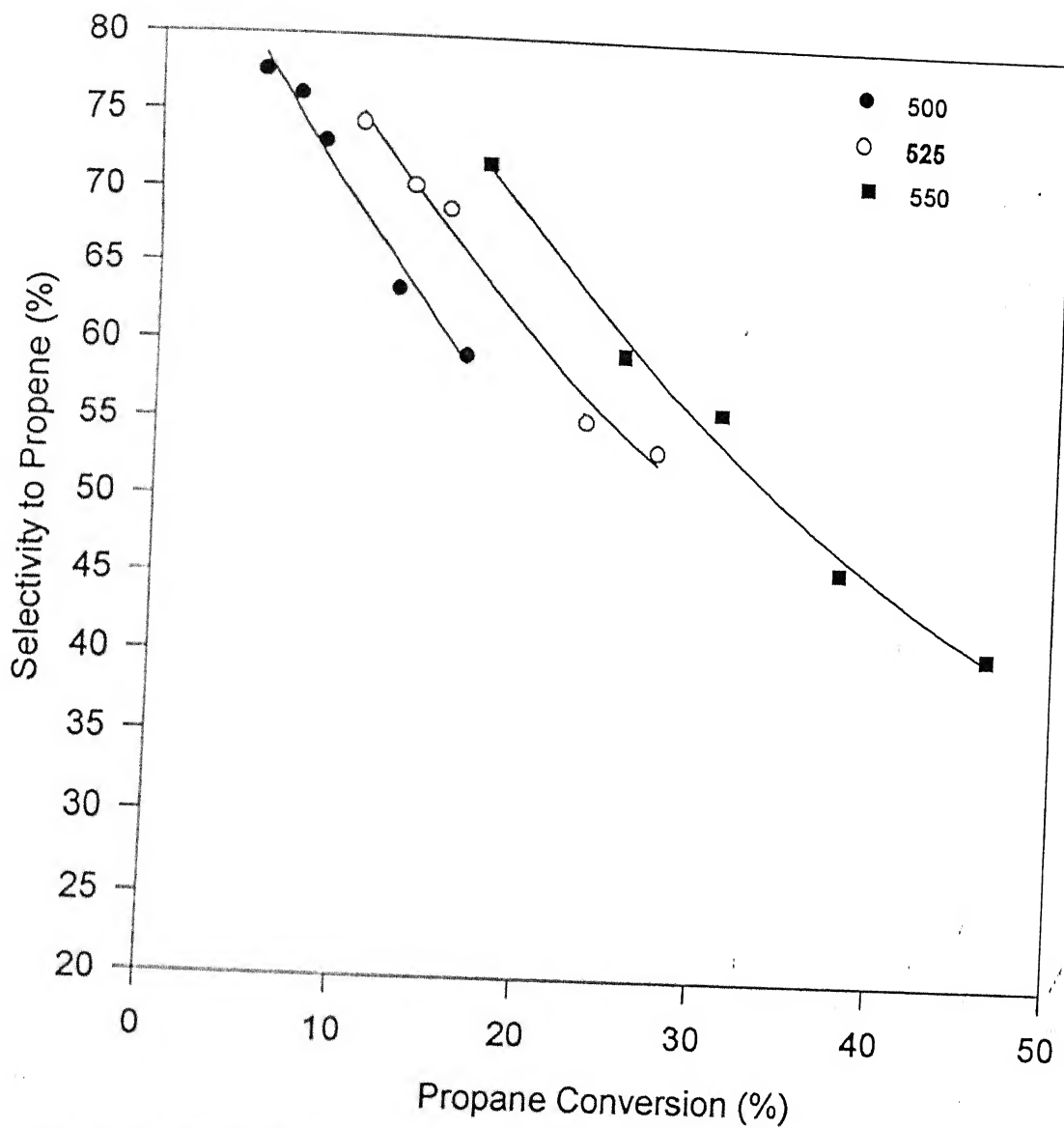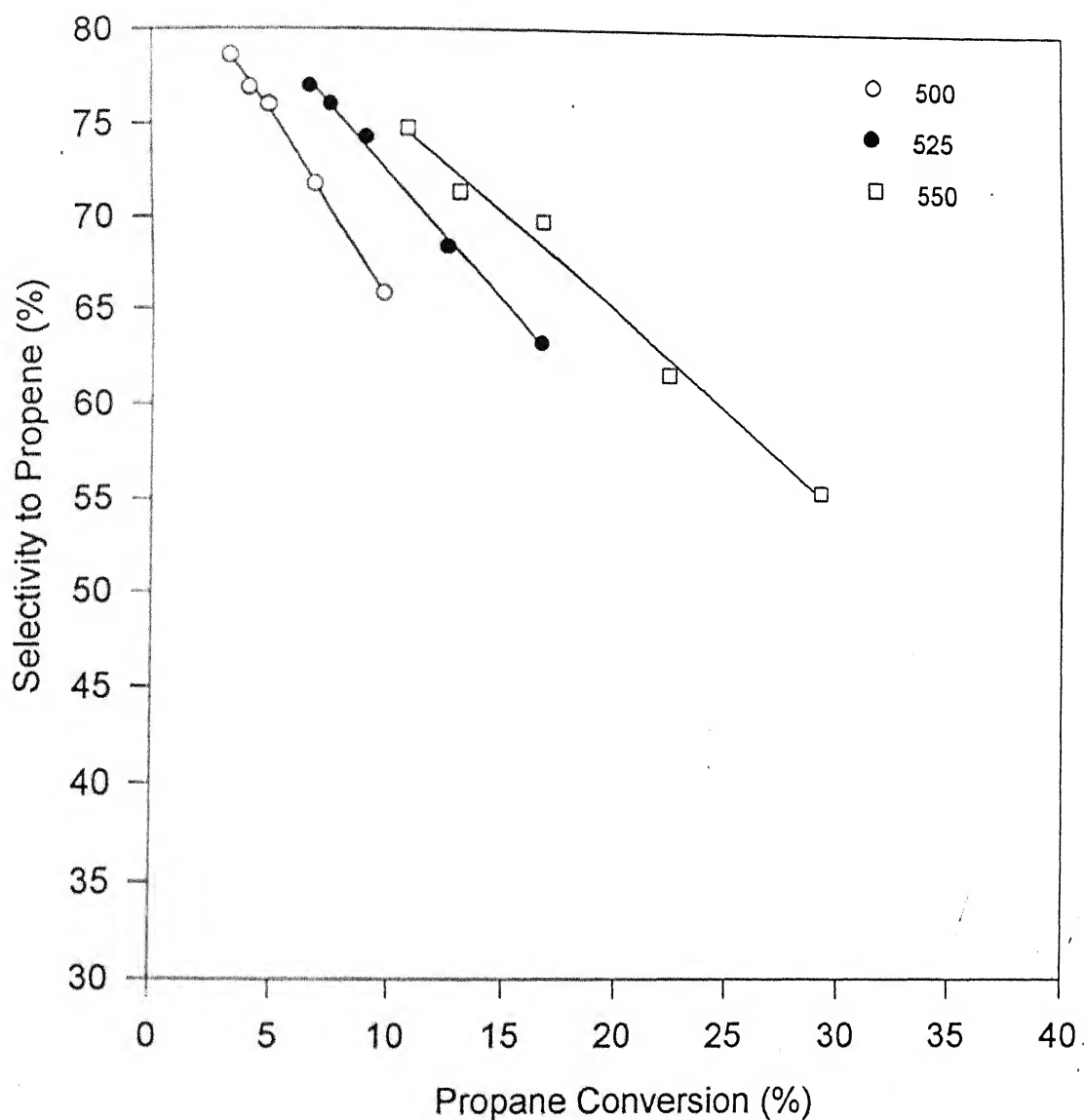
Figure 5.6 Variation of propene selectivity with propane conversion at different temperatures for $Mo_{0.6}V_1Mg_9O_x$

Figure 5.7 Variation of propene selectivity with propane

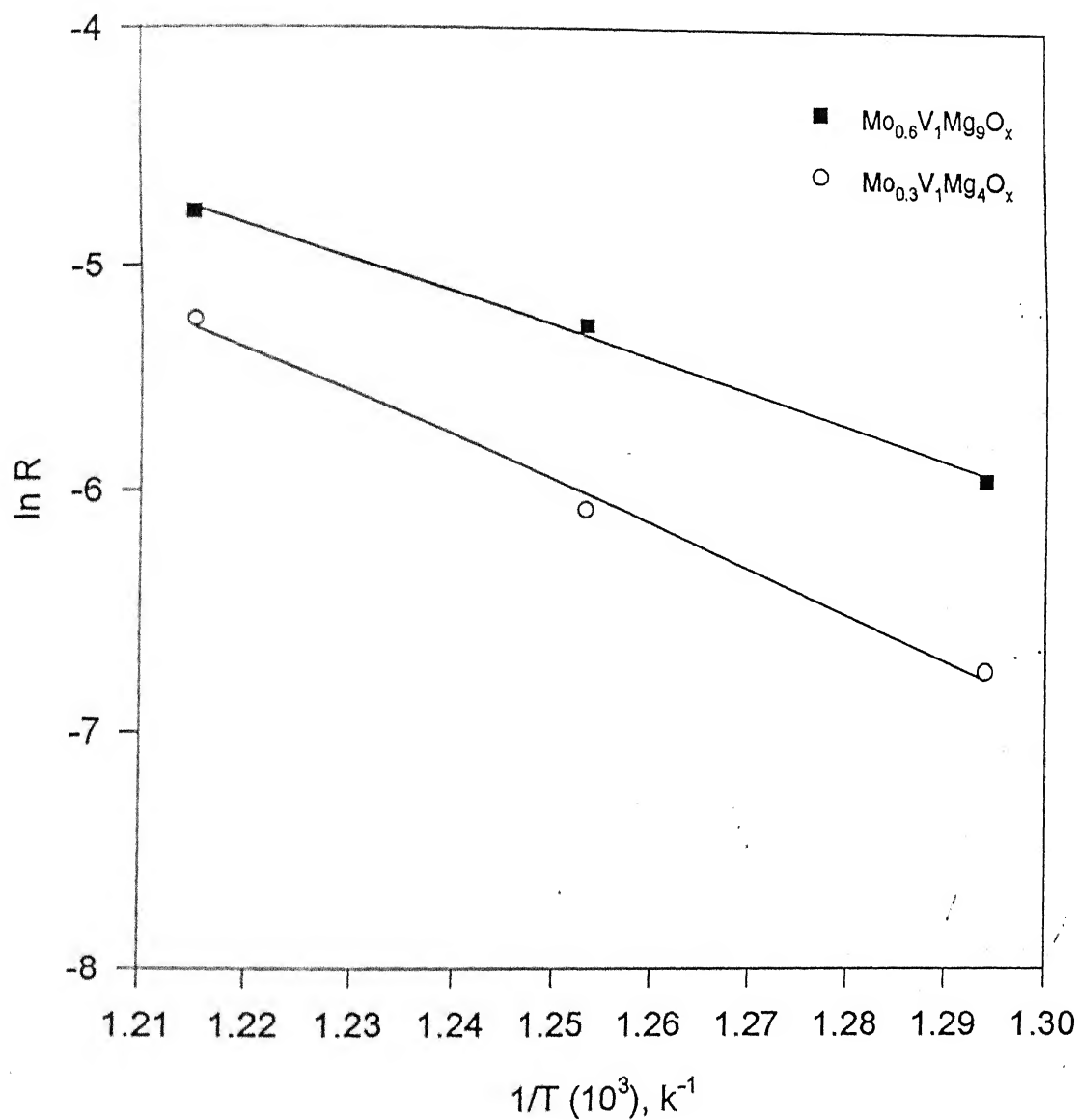conversion at different temperatures on $Mo_{0.3}V_1Mg_4O_x$

Figure 5.8 Arrhenius plots for the catalysts $Mo_{0.6}V_1Mg_9Ox$ and $Mo_{0.3}V_1Mg_4O_x$

5.2.3. Deactivation of the catalysts

At the highest temperature studied (550 ^{0}C), the color of the used binary catalysts having low vanadium content ($V_1Mg_4O_x$ and $V_1Mg_9O_x$) was found to be black (The fresh catalysts were light yellow in color). This color change was due to the coke deposition on the catalyst. Moreover, for some catalysts it was observed that the conversion decreased for consecutive runs taken at an interval of 2 hr under the same conditions. This clearly showed that the catalysts were deactivating with time, especially at 550 ^{0}C. On the other hand, it was noticed that for Mo-doped catalysts, the coke deposition was less and for catalysts with a Mo/V atomic ratio of 0.6 and higher, there was no change in color. To further investigate the effect of Mo doping on catalyst deactivation, the change in conversion with time was measured for $V_1Mg_9O_x$ and $Mo_{0.6}V_1Mg_9O_x$ at 550 ^{0}C. W/F$_{A0}$ was adjusted such that the initial conversion for both the catalysts was approximately the same (~45.0±3 %). The variation of catalyst activity, calculated as the ratio of the conversion at any time to the initial conversion, is shown in Figure 5.9 for both the catalysts. As can be seen, the decline in activity of $Mo_{0.6}V_1Mg_9O_x$ is much less than for the undoped catalyst. A possible reason for the lower coke deposition on the doped catalyst could be the catalytic effect of Mo on the coke oxidation reaction. However, more investigation is required to fully explain the lower rate of catalyst deactivation.
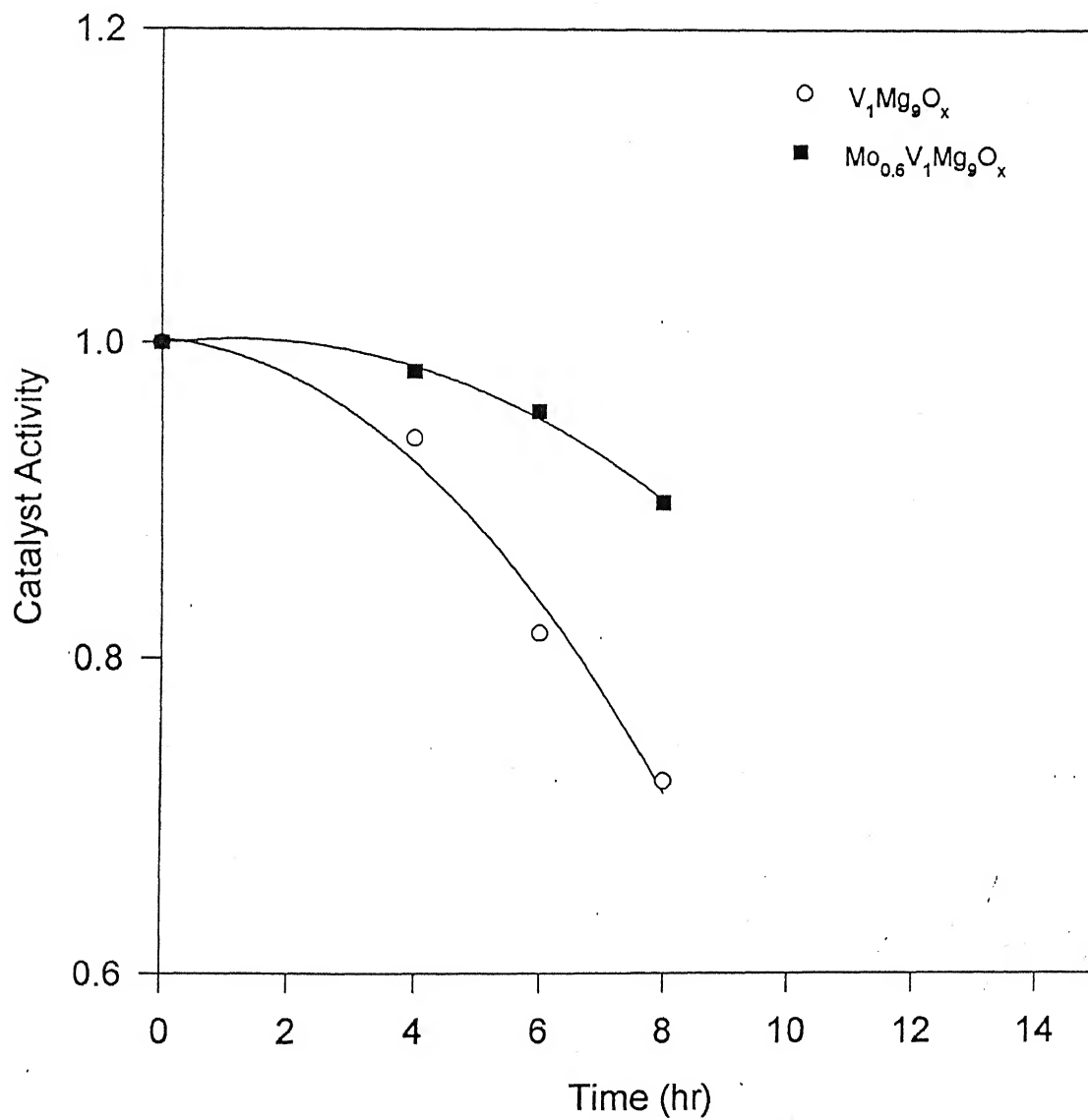
Fig 5.9 Deactivation of the catalyst with time

5.3. Discussion

As the above results show, the activity of the Mo-doped catalysts decreased with increasing molybdenum content. One reason for this can be the decrease in reducibility of the catalyst with increasing molybdenum content. This was confirmed earlier by the TPR study. The reduction temperatures of the molybdenum doped catalysts were found to be higher than those of the undoped catalysts, which indicate that the reducibility of the vanadium species decreases with increasing Mo content. Since a correlation between the reducibility of active sites and the catalytic activity for ODH reactions is generally observed on vanadium based catalysts [34, 35], the lower activity of the Mo-doped samples could be explained by a decrease in reducibility of the active sites, i.e. VO_4 tetrahedra.

One more reason for the decrease in catalytic activity of the molybdenum doped catalysts could be the decrease in their surface areas. With a decrease in the total surface area, the number of active sites is likely to be lower. However, the experimental results of the present study show that the rate of propane consumption, calculated as gmoles reacted/m^2-hr, decreased from 0.017 to 0.0069 as the Mo content of the catalyst was increased from 0.1 to 1.0. Thus the lower catalytic activity of the molybdenum doped catalysts can not be explained solely by the reduction in surface area.

On the other hand, the increase of selectivity to propene with molybdenum loading can be related to the variation of non-selective sites on the surface of the catalyst. Studies on V-Mg-O catalyst [35] have shown that the magnesia support catalyses the non-selective oxidation of alkanes to carbon oxides. The increase in the selectivity could be due to the decrease in the number of basic sites due to the support, i.e. magnesia and the formation of new sites related to molybdenum. In a related study of ODH of n-butane on Mo doped V-Mg-O catalysts [24], the results obtained from FTIR and XPS characterization showed that the concentration of the non-selective Mg^{2+} sites

68

on the catalyst surface reduced when Mo was incorporated in the catalyst. For our studies, XPS was not available and therefore the surface concentration of V, Mg, and Mo could not be obtained.

One more reason for the increase of selectivity of the Mo doped catalysts could be due to the change in activation energies of the ODH reactions due to the incorporation of molybdenum. The participation of the lattice oxygen in ODH of propane is well known and the catalyst reducibility can modify the rate of alkane activation and selective oxidation. As the reduction temperatures of the catalysts fall in the range of catalytic reactions, the activation energies of the oxidative dehydrogenation reaction may be influenced by the molybdenum loading.

6

Conclusions and Recommendations

6.1. Conclusions

Based on the results of the present study, the following conclusions can be made:

1. The activity of the binary V-Mg-O catalysts depends on the vanadium content. Of all the binary catalysts, the highest activity was obtained on $V_1Mg_9O_x$ catalyst, with a V_2O_5 content of 20wt%.

2. In the range of Mo/V atomic ratio of 0.1 to 1.0, addition of molybdenum to the V-Mg-O catalyst causes a decrease in the catalytic activity of the catalyst and this can be explained by the decrease in reducibility of V ions. The higher the Mo content, the lower is the activity.

3. Addition of molybdenum caused the increase in the selectivity of the catalyst in the ODH of propane. Till a Mo/V atomic ratio of 0.6, an increase in the Mo content of the catalyst, increases the selectivity of propene in the ODH reaction. Further increase in Mo/V atomic ratio does not have any appreciable effect on the selectivity (refer Figure 5.2). This can be explained by the decrease in the number of non-selective sites, due to the incorporation of molybdenum.

4. At a fixed conversion, the selectivity to propene can be increased by operating at a higher temperature. This can be explained by the higher activation energy of the ODH reaction compared to the activation energies for the formation of carbon oxides.

5. Mo doped V-Mg-O catalysts deactivate at a lower rate in comparison to the undoped V-Mg-O catalysts.

6.2. Recommendations

The following recommendations are proposed for the further study:

1. More detailed characterization of the catalysts should be made using techniques such as XPS, Raman spectra etc. so that the effect of surface concentration of different species on the activity and selectivity can be determined.

2. Role of acid-base properties of the catalyst on the performance of the ODH reactions should be studied.

3. A quaternary catalytic system incorporating the active additive in Mo-V-Mg-O should be studied.

References

[1] A. Corma, J.M. Lopez-Nieto, N. Paredes, M. Perez, Y. Shen, H. Cao, S.L. Suib, "Oxidative dehydrogenation of propane over supported vanadium oxide catalysts", *Stud. Surf. Sci. Catal.*, **72**, 1992, 213-220.

[2] Barbara G.S., "Active centres on vanadia-based catalysts for selective oxidation of hydrocarbons", *Appl. Catal. A*, **157**, 1997, 409-420.

[3] S. Albonetti, F. Cavani, F. Trifiro, "Key aspects of catalyst design for the selective oxidation of paraffins", *Cat. Rev. Sci. Eng.*, **38**, 4, 1996, 413-438.

[4] H.H. Kung, "Oxidative dehydrogenation of light (C_2 to C_4) alkanes", *Advances in Catalysis*, **40**, 1994, 1-37.

[5] E.A. Mamedov, V.C. Coberan, "Oxidative dehydrogenation of lower alkanes on vanadium oxide based catalysts. The present state of the art and outlooks", *Appl. Catal. A*, **127**, 1995, 1-40.

[6] D. Siew Hew Sam, V. Soenen, J.C. Volta, "Oxidative dehydrogenation of propane over V-Mg-O catalysts", *J. Catal.*, **123**, 1990, 417-435.

[7] M.A. Chaar, D. Patel, H.H. Kung, "Selective oxidative dehydrogenation of propane over V-Mg-O catalysts", *J. Catal.*, **109**, 1988, 463-467.

[8] A.G. Ruiz, I.R. Ramos, J.L.G. Fierro, V. Soenen J.M. Herrmann, J.C. Volta, "Nature of surface sites in the selective oxide hrdogenation of propane over V-Mg-O catalysts", *Stud. Surf. Sci. Catal.*, **72**, 1992, 203-212.

[9] A. Corma, J.M. Lopez Nieto, N. Paredes, "Influence of preparation methods of V-Mg-O catalysts on their catalytic properties for the oxidative dehydrogenation of propane", *J. Catal.*, **144**, 1993, 425-438.

[10] X. Gao, P. Ruiz, Q. Xin, X. Guo, B. Delmon, "effect of coexistence of magnesium vanadate phases in the selective oxidation of propane to propene", *J. Catal.*, **148**, 1994, 56-67.

[11] S.R.G. Carrazan, C. Peres, J.P. Bernard, M. Ruwet, P. Ruiz, B. Delmon, "Catalytic synergy in the oxidative dehydrogenation of propane over MgVO catalysts", *J. Catal.*, **158**, 1996, 452-476.

[12] R. Burch, E.M. Crabb, "Homogeneous and heterogeneous contributions to the oxidative dehydrogenation of propane on oxide catalysts", *Appl. Catal.*, **100**, 1993, 111-130.

[13] K.T. Nguyen, H.H. Kung, "Generation of gaseous radicals by a V-Mg-O catalyst during oxidative dehydrogenation of propane", *J. Catal.*, **122**, 1990, 415-428.

[14] B. Delmon, P. Ruiz, S.R.G. Carrozan, S. Korili, M.A. Vincent Rodriguez, Z. Sobalik in M. Absi-Halabi et al., Eds., *Catalysts in Petroleum refinning and Petrochemical Industries 1995*, Elsevier, 1996.

[15] T.C. Watting, G. Deo, K. Seshan, I.E. Wachs, J.A.Lercher, "Oxidative dehydrogenation of propane over niobia supported vanadium oxide catalysts", *Catalysis Today*, **28**, 1996, 139-145.

[16] Young Seek Yoon, Wataru Ueda, Yoshihiko Moro-oka, "Oxidative dehydrogenation of propane over molybdate catalysts", *Catal. Letters*, **35**, 1995, 57-64.

[17] R.X. Valenzuela, E.A. Mamedov, V. Cortes Corberan, "Effect of different additives on the performance of V-Mg-O catalysts in the oxidative dehydrogenation of propane" *React. Kinet. Catal. Lett.*, Vol. 55, No. 1, 213-220.

[18] R. Juarez Lopez, N.S. Godjayeva, V. Cortes Corberan, J.L.G. Fierro, E.A. Mamedov, "Oxidative dehydrogenation of ethane on supported vanadium-containing oxides", *Appl. Catal. A*, **124**, 1995, 281-296.

[19] R.X Valenzuela, J.L.Z. Fierro, V. Cortes Corberan, E.A. Mamedov, "Ethane oxidehydrogenation selectivity and reducibility of mixed NiVSb oxides", *Catal. Letters*, **40**, 1996, 223-228.

[20] E.M. Thorsteinson, T.P. Wilson, F.G. Young, P.H. Kasai, "The Oxidative Dehydrogenation of Ethane over Catalysts Containing Mixed Oxides of Molybdenum and Vanadium", *J. Catal.*, **52**, 1978, 116-132.

[21] R. Burch, R. Swarnakar, "Oxidative dehydrogenation of ethane on vanadium-molybdenum oxide and vanadium-niobium-molybdenum oxide catalysts", *Applied Catalysis*, **70**, 1991, 129-148.

[22] D.L. Stern, J.N. Michaels, L. DeCanl, R.K. Graselli, "Oxy-dehydrogenation of n-butane over promoted Mg-V-O based catalysts", *Appl. Catal. A*, **153**, 1997, 21-30.

[23] D. Bhattacharya, Shyamal K. Bej and Musti S. Rao, "Oxidative dehydrogenation of n-butane to butediene, Effect of different promoters on the performance of vanadium-magnesium oxide catalysts", *Appl. Catal. A*, **87**, 1992, 29-43.

[24] A. Dejoz, J.M. Lopez Nieto, F. Marquez, M.I. Vazquez, "The role of molbdenum in Mo doped V-Mg-O catalysts during the oxidative dehydrogenation of n-butane", *Appl. Catal. A*, **180**, 1999, 83-94.

[25]   W. Oganowski, J. Hanuza, H. Drulis, W. Mista, L. Macalik, "Promotional effect of molybdenum, chromium and cobalt on a V-Mg-O catalyst in the oxidative dehydrogenation of ethylbenzene to styrene", *Appl. Catal. A*, **136**, 1996, 143-159.

[26]   R.H.H. Smits, "The oxidative dehydrogenation of propane", Ph. D. Thesis, Twente University, Netherlands, 1994.

[27]   P. Viparelli, P. Ciambelli, L. Lisi, G. Ruoppolo, G. Russo, J.C. Volta, "Oxidative dehydrogenation of propane over vanadium and niobium oxides supported catalysts", *Appl. Catal. A*, **184**, 1999, 291-301.

[28]   G.S.S. Murty, "Oxidative dehydrogenation of propane on V-Mg-O catalyst. Effect of molybdenum and boron", *M. Tech. Thesis*, I.I.T. Kanpur, 1998.

[29]   S.B. Malge, "Oxidative Dehydrogenation of Propane on Vanadia-based ternary metal oxide catalysts", *M. Tech. Thesis*, I.I.T. Kanpur, 1999.

[30]   A. pantazidis, C. Mirodatos, "Identification of Active Sites and Structure Sensitivity of the oxidative dehydrogenation of propane over Vanadium Magnesium Oxide Catalysts", in B.K. Warren, S.T. Oyama, Eds., *Heterogeneous Hydrocarbon Oxidation*, ACS Symp. Ser. **638**, American Chemical Society, Washington DC, 1996, 207-222.

[31]   W.F. McClune, Ed., Powder Diffraction File, Inorganic Volume, 1985, Published by Joint Committee on Powder Diffraction Standard, Swarthmore, USA.

[32]   A. Baiker, M.A. Kohler, "Characterization of catalysts", in N.P. Cherimisinoff, Ed., Handbook of Heat and Mass Transfer Volume 3: Catalysis, Kinetics, and Reactor Engineering, Gulf Publishing Company, 1989.

[33]   D. Patel, M.C. Kung, H.H. Kung, in *Proc. 9th International Congress on Catalysis*, M.J. Phillips, M. Ternan, eds., Chemical Institute of Canada, Ottawa, 1988, **4**, 1553.

[34]   G. Deo, I.E. Wachs, "Effect of additives on the structure and reactivity of the surface vanadium oxide phase in V_2O_5/TiO_2 catalysts", *J. Catal.*, **146**, 1994, 335-345.

[35]   P. Concepcion, J.M. Lopez Nieto, J. Perez-Pariente, "Oxidative dehydrogenation of propane on VAPO-5, $V_2O_5/ALPO_4$-5 and V_2O_5/MgO catalysts. Nature of selective sites", J. Mol. Catal. A., 99, 1995, 173-182.

[36]   L.E. Cadus, M.F. Gomez, M.C. Abello, "Synergy effects in the oxidative dehydrogenation of propane over $MgMoO_4$-MoO_3 catalysts", *Catal. Letters*, **43**, 1997, 229-233.

Appendix 1

Calibration factors were used in calculating the mole ratios of different compounds in the product mixture. It was defined as

$$\text{Calibration factor of i with respect to i', } K_{ii'} = \frac{\dfrac{\text{mole fraction of i in the standard mixture}}{\text{mole fraction of i' in the standard mixture}}}{\dfrac{\text{Area of i}}{\text{Area of i'}}}$$

1. Calibration factor for oxygen

For the calculation of calibration factor of oxygen with respect to nitrogen, air was used as the standard mixture.

Detector: TCD

Column: Molecular Sieve 5A .

Carrier gas (Helium) flow rate: 30 cc/min

Temperatures: Oven: $50\,^0C$; Injector: 70^0C; Detector: $200\,^0C$;

Calibration factor of oxygen with respect to nitrogen = 1.0024

2. Calibration factors for CO, CO_2 and C_3H_6

Calibration factors of CO, CO_2 and C_3H_8 were calculated using standard gas mixture (Multi tech, New Delhi) of following composition in mol%

CO: 0.55; CO_2: 1.9; CH_4: 0.0081 C_2H_6: 0.008;

C_2H_2: 0.0086; C_3H_6: 0.71; C_3H_8: 3.1; O_2: 2.48;   Balance N_2;

Detector: FID

Column: Carbo sphere

Carrier gas (Nitrogen) flow rate: 30 cc/min

Temperatures: Oven: Programm mode

                    Initially 20 min at 45 ^{0}C for the detection of CO, CO_2

                    Heated up to 200 ^{0}C at a rate of 20 ^{0}C/min

                    40 min at 200 ^{0}C to detect C_3H_6 and C_3H_8

            Injector: 100 ^{0}C; Detector: 150 ^{0}C

            Methanizer: 310 ^{0}C

Calibration factor of CO with respect to C_3H_8 = 2.2815

Calibration factor of CO_2 with respect to C_3H_8 = 4.1081

Calibration factor of C_3H_6 with respect to C_3H_8 = 1.1407